
Graph Neural Network with Local Frame for Molecular Potential Energy Surface

Xiyuan Wang¹ Muhan Zhang^{1,2,*}

¹Institute for Artificial Intelligence, Peking University

²Beijing Institute for General Artificial Intelligence
wangxiyuan@pku.edu.cn, muhan@pku.edu.cn

Abstract

Modeling molecular potential energy surface is of pivotal importance in science. Graph Neural Networks have shown great success in this field, especially those using rotation-equivariant representations. However, they either suffer from a complex mathematical form or lack theoretical support and design principle. To avoid using equivariant representations, we introduce a novel *local frame* method to molecule representation learning and analyze its expressive power. With a frame and the projection of equivariant vectors on the frame, GNNs can map the local environment of an atom to a scalar representation injectively. Messages can also be passed across local environments with frames' projection on frames. We further analyze when and how we can build such local frames. We prove that local frames always exist when the local environments have no symmetry, as is often the case in molecular dynamics simulations. For symmetric molecules, though only degenerate frames can be built, we find that the local frame method may still achieve high expressive power in some common cases due to the reduced degrees of freedom. Using only scalar representations allows us to adopt existing simple and powerful GNN architectures. Our model outperforms a range of state-of-the-art baselines in experiments. Simpler architectures also lead to higher scalability. Our model only takes about 30% inference time compared with the fastest baseline.

1 Introduction

Prediction of molecular properties is widely used in fields such as material searching, drug designing, and understanding chemical reactions [Schmitz et al., 2019]. Among properties, potential energy surface (PES) [Lewars, 2016], the relationship between the energy of a molecule and its geometry, is of pivotal importance as it can determine the dynamics of molecular systems and many other properties. Many computational chemistry methods have been developed for the prediction, but few of them can achieve both high precision and scalability.

In recent years, machine learning (ML) methods, which are both accurate and efficient, have emerged. Among these ML methods, Graph Neural Networks (GNNs) are especially promising. In the past few years, they have improved continuously [Schutt et al., 2017, Schütt et al., 2017, Klicpera et al., 2020, Anderson et al., 2019, Schütt et al., 2021, Gasteiger et al., 2021, Batzner et al., 2021, Thölke and Fabritiis, 2022] and achieved state-of-the-art performance on many benchmark datasets. Compared with popular GNNs used in other graph tasks [Kipf and Welling, 2017], these GNNs need a lot of special designs, as molecules are more than a graph composed of merely nodes and edges. Atoms are in the continuous three-dimensional space, and the prediction targets like energy are sensitive to the position of atoms. Therefore, to model molecules, GNNs must include geometric information.

*Corresponding author: Muhan Zhang (muhan@pku.edu.cn).

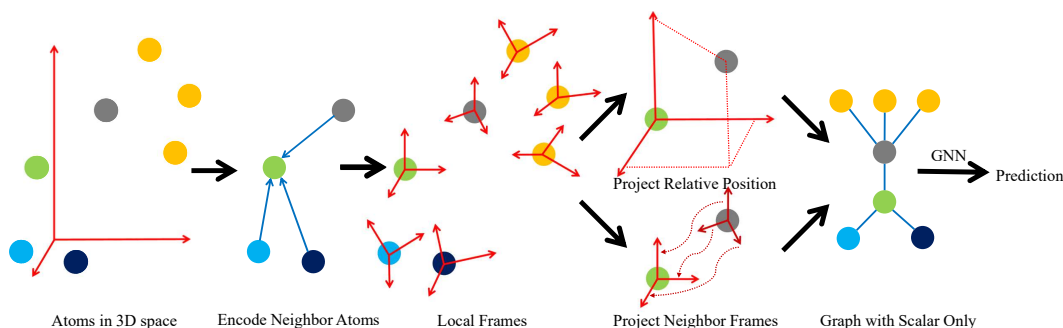


Figure 1: An illustration of our model. A local frame is generated for each atom, which is used to encode the geometric information of its neighborhood into scalars. Then an ordinary GNN is applied. Moreover, for generalization, symmetry of the predicted properties must be taken into consideration. For example, if an isolated molecule rotates, the energy will not change. Thus, the prediction of a model should not change either.

Various theories and models have been proposed to capture the target’s symmetry. Equivariant representations are widely used in these approaches. Among them, some models [Thomas et al., 2018, Batzner et al., 2021, Anderson et al., 2019] use irreducible representations of the $SO(3)$ group and suffer from complex mathematical form and low scalability. Other models [Schütt et al., 2021, Thölke and Fabritiis, 2022] manually design equivariant functions for vector and scalar representations and achieve outstanding performance. However, to deal with two kinds of representations, functions for these two kinds must be defined separately, and complex operation is needed to mix the information contained in the two kinds of representations. Furthermore, the design is often complicated and ad hoc due to the lack of design principle and theoretical support, hampering these models’ scalability and comprehensibility. In contrast, models using only invariant representations [Schütt et al., 2017, Klicpera et al., 2020, Gasteiger et al., 2021] can use the elegant architectures and theories of ordinary GNNs, though they are usually less expressive than those using equivariant representations. Therefore, we wonder whether equivariant representations can be replaced with invariant representations while keeping the high expressive power.

In this work, we propose a simple, scalable, yet expressive GNN for molecular property prediction. As shown in Figure 1, our model first produces a local frame for each atom based on its local environment. Then it projects the relative positions and frames of neighbor atoms on the frame to create a graph with only scalar features. Finally, a normal GNN can work on the graph to produce a prediction. Our model outperforms all baselines on a majority of the targets in the MD17 and QM9 datasets. It also achieves three times higher inference speed than the fastest baseline on the PES task.

2 Related work

We can classify existing ML models for PES into two classes: manual descriptors and GNNs.

Manual Descriptor. These models first use manually designed functions with few learnable parameters to convert one molecule to a descriptor vector and then feed the vector into some ordinary ML models like kernel regression [Rupp et al., 2012, Chmiela et al., 2019, Christensen et al., 2020] and neural networks [Behler and Parrinello, 2007, Smith et al., 2017, Zhang et al., 2018] to produce the prediction. Compared with GNNs, these methods are more scalable and data-efficient. However, they are less accurate and cannot process variable-size molecules or different kinds of atoms due to the hard-coded descriptors. Our model outperforms one state-of-the-art model of them [Christensen et al., 2020] on the MD17 dataset with the same data split while using a more flexible GNN architecture.

GNN. These GNNs mainly differ in the way to incorporate geometric information. Schütt et al. [2017] and Schütt et al. [2017] only consider the distance between atoms. Klicpera et al. [2020] introduce angular features to describe the direction of interaction, and Gasteiger et al. [2021] further use dihedral angles. All these models use rotation-invariant geometric features only, so we call them *invariant models*. Though it is theoretically expressive, GemNet [Gasteiger et al., 2021] has high time complexity of up to $O(Nn^3)$, where n is the number of atoms in the neighborhood of one atom and N is the number of atoms in the molecule. Recent works have also utilized rotation-equivariant features. Some [Anderson et al., 2019, Thomas et al., 2018, Batzner et al., 2021] are based on irreducible

representations of the $SO(3)$ group. Though having certain theoretical guarantees, these models have complex formulations in their full forms and are hard to implement. Their scalability also suffers from special functions used for group representations. Other works [Schütt et al., 2021, Thölke and Fabritiis, 2022] model equivariant interactions in Cartesian space using both invariant representations and *vector representations*, which are sequences of 3-vectors rotating with the molecule. They are much simpler and achieve state-of-the-art performance with low time complexity of only $O(Nn)$. However, these models have no theoretical guarantees. Their architectures are also complex due to different sets of functions that must be designed separately for different input and output types. Our work avoids both irreducible representations and vector representations. We introduce an $O(3)$ -equivariant frame and project all equivariant features on the frame injectively, thus deserting vector representations while keeping the expressive power. The proposed method is simple and scalable. Though it has the same time complexity $O(Nn)$ as existing state-of-the-art models, our model only needs to process scalar and has no computation overhead for transforming vector or mixing scalar and vector.

Besides potential energy surface models, methods designed for other molecular tasks and point cloud also use GNNs to capture geometric information. Some of them [Du et al., 2022, Satorras et al., 2021, Luo et al., 2021, Huang et al., 2022] also use the term "frame" or some designs similar to frame. However, these methods are quite different from ours. The most notable difference is that even using frame, existing models still keep vector features, while our model completely deserts vector features and only operates on a vanilla scalar graph after projection. This can greatly simplify the architecture without losing expressive power. The comparison is detailed in Appendix I. Moreover, these methods can be categorized into models using both invariant representations and vector representations. Our model can beat the representative methods [Schütt et al., 2021, Thölke and Fabritiis, 2022] of this kind in both accuracy and scalability on potential energy surface prediction tasks.

3 Preliminaries

Modeling PES. PES is the relationship between molecular energy and geometry. Given a molecule with N atoms, our model takes the kinds of atoms $z \in \mathbb{Z}^N$ and the three-dimensional coordinates of atoms $\vec{r} \in \mathbb{R}^{N \times 3}$ as input to predict the energy $\hat{E} \in \mathbb{R}$ of this molecule. It can also predict the force on atoms $\hat{F} \in \mathbb{R}^{N \times 3} = -\nabla_{\vec{r}} \hat{E}$. With PES, many properties can be calculated by molecular dynamics (MD) simulations, which has been well studied in the computational chemistry field and is not our focus. Nevertheless, our model can also predict other molecular properties directly.

Equivariance. We define equivariant and invariant functions the same as in [Villar et al., 2021].

Definition 3.1. Given a function $h : \mathbb{X} \rightarrow \mathbb{Y}$ and a group G acting on \mathbb{X} and \mathbb{Y} as \star . We say that h is

$$G\text{-invariant:} \quad \text{if } h(g \star x) = h(x), \quad \forall x \in \mathbb{X}, g \in G \quad (1)$$

$$G\text{-equivariant:} \quad \text{if } h(g \star x) = g \star h(x), \quad \forall x \in \mathbb{X}, g \in G \quad (2)$$

The energy is invariant to the permutation of atoms, coordinates' translations, and coordinates' orthogonal transformations (rotations and reflections). The architecture of GNN naturally keeps the permutation invariance. As the relative position $\vec{r}_{ij} = \vec{r}_i - \vec{r}_j$, which is invariant to translation, is usually used as the input to GNNs, the translation invariance can also be ensured easily. So we focus on orthogonal transformations. Orthogonal transformations of coordinates form the group $O(3) = \{Q \in \mathbb{R}^{3 \times 3} \mid QQ^T = I\}$, where I is the identity matrix. Representations are considered as **functions of z and \vec{r}** . Below we define *scalar representations* and *vector representations*, respectively.

Definition 3.2. Representation s is called a **scalar representation** if $s(z, \vec{r}) = s(z, \vec{r}o^T), \forall o \in O(3), z \in \mathbb{Z}^N, \vec{r} \in \mathbb{R}^{N \times 3}$. Representation \vec{v} is called a **vector representation** if $\vec{v}(z, \vec{r})o^T = \vec{v}(z, \vec{r}o^T), \forall o \in O(3), z \in \mathbb{Z}^N, \vec{r} \in \mathbb{R}^{N \times 3}$.

Scalar and vector representations are also called invariant and equivariant representations in some previous work [Thölke and Fabritiis, 2022]. Sometimes we simply call them scalars and vectors. Note that the scalars in our definition are not restricted to one number, and the vectors may not only be of shape $(1, 3)$. In Lemma 3.1, we introduce some basic operations of scalars and vectors.

Lemma 3.1.

- (Function of scalar) Any function of scalar s will produce a scalar.

- (Scale of vector) Let s denote a scalar of shape (F) , \vec{v} denote a vector of shape $(F, 3)$. We define $s \circ \vec{v}$ to output a matrix of shape $(F, 3)$, whose (i, j) th element is $s_i \vec{v}_{ij}$. When \vec{v} is of shape $(1, 3)$, we first broadcast it along the first dimension. Then the output is also a vector representation.
- (Projection) Let \vec{v}_1, \vec{v}_2 denote two vectors of shape $(F_1, 3)$ and $(F_2, 3)$, respectively. The projection of \vec{v}_1 to \vec{v}_2 , denoted as $P(\vec{v}_1, \vec{v}_2) := \vec{v}_1 \vec{v}_2^T$, is a scalar of shape (F_1, F_2) .
- (Inner product) Let \vec{v}_1, \vec{v}_2 denote two vectors of shape $(F, 3)$. The inner product $\langle \vec{v}_1, \vec{v}_2 \rangle := \text{diag}(P(\vec{v}_1, \vec{v}_2))$ is a scalar of shape (F) .

Local Environment. Most message passing frameworks for PES encode the *local environment* of each atom in each message passing layer as defined in Definition 3.3.

Definition 3.3. Let r_{ij} denote $\|\vec{r}_{ij}\|$. The **local environment** of atom i is $LE_i = \{(s_j, \vec{r}_{ij}) | r_{ij} < r_c\}$, the set of scalar atom features s_j and relative positions \vec{r}_{ij} of atoms j within the sphere centered at i with cutoff distance r_c , where r_c is usually a hyperparameter.

We just let the scalar feature s_j be initialized with the kind of atom z_j , but it is not restricted to that. In this work, orthogonal transformation of a set/sequence means transforming each element in the set/sequence, respectively. For example, an orthogonal transformation o will map $\{(s_j, \vec{r}_{ij}) | r_{ij} < r_c\}$ to $\{(s_j, \vec{r}_{ij} o^T) | r_{ij} < r_c\}$.

4 Local frame

In general, our model projects all vector representations of neighbors on the local frame of each atom to enable using ordinary GNNs on a graph with scalars only. This section first illustrates how local frames capture geometric information and then explains how to build local frames. With a frame, we can easily convert geometric features into scalars without information loss and achieve high expressive power with ordinary GNNs.

4.1 Rethinking vector representations

Though vector representations have been used for a long time, it is still unclear how to ideally transform them. Existing methods [Schütt et al., 2021, Thölke and Fabritius, 2022, Deng et al., 2021, Villar et al., 2021] either have no theoretical guarantee or tend to use too many parameters, resulting in possible redundancy of computation. In this study, we ask a fundamental question, can we totally give up vector representations during the message passing? The motivation is that, given scalars only, we have mature ordinary GNN architectures with guaranteed expressive power. It also eliminates the complex conversions between scalars and vectors.

Assume there exist three linearly independent vector representations in $\mathbb{R}^{1 \times 3}$ forming a frame $\vec{E} \in \mathbb{R}^{3 \times 3}$, whose rows are equivariant to orthogonal transformations. We will discuss how to generate the frame in Section 4.3. We define the projection function on the frame \vec{E} as follows:

$$P_{\vec{E}}(\vec{x}) := P(\vec{x}, \vec{E}) = \vec{x} \vec{E}^T. \quad (3)$$

Given the frame \vec{E} , the projection will contain all the information of the input vector \vec{x} as shown in Proposition 4.1.

Proposition 4.1. $P_{\vec{E}}$ is a bijective function, which maps a vector shape $(F, 3)$ to a scalar of shape $(F, 3)$. Its inverse function $P_{\vec{E}}^{-1}$ maps a scalar of shape $(F, 3)$ to a vector of shape $(F, 3)$.

Therefore, we can use $P_{\vec{E}}$ and $P_{\vec{E}}^{-1}$ to map between scalar representations and vector representations. Moreover, it allows us to express any equivariant function acting on vectors with an invariant function acting on scalars as shown in the following proposition.

Proposition 4.2. Given *any* equivariant function g , there exists a function $\tilde{g} = P_{\vec{E}} \cdot g \cdot P_{\vec{E}}^{-1}$ which takes scalar representations as input and outputs scalar representations, where \cdot means function composition. And $g = P_{\vec{E}}^{-1} \cdot \tilde{g} \cdot P_{\vec{E}}$.

We can use an MLP to approximate the function \tilde{g} and thus achieving **universal approximation** for all $O(3)$ -equivariant functions. This demonstrates one advantage of the frame method—we can

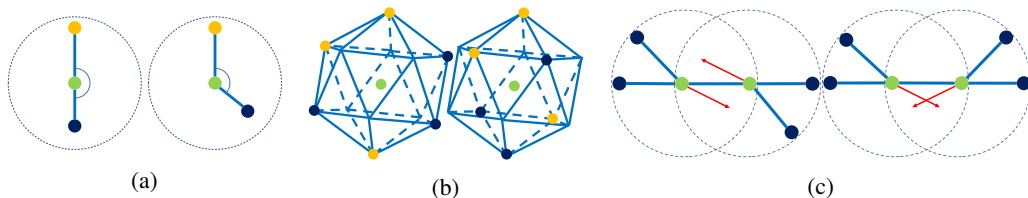


Figure 2: The green balls in the figure are the center atoms. We use balls with different colors to represent different kinds of atoms. (a) SchNet cannot distinguish two local environments due to the inability to capture angle. (b) DimeNet cannot distinguish two local environments with the same set of angular embeddings. Blue lines form a regular icosahedron and help visualization. The center atom is at the symmetrical center of the icosahedron. (c) Some invariant GNN models fail to pass the orientation information. However, including projection of frame vectors can solve this problem (right). We only show one vector (red) to represent the frame for simplicity. As a part of the molecule rotates, the $O(3)$ -equivariant local frame will also rotate, leading to a different projection.

transform vectors to scalars in the beginning, fully operate on the scalar space without losing any expressive power. We can also transform scalars back to vector prediction if needed.

4.2 How frames boost the expressive power

Encoding local environment. On the one hand, most GNNs for PES only pass messages to the center atom from atoms within the sphere of radius r_c . Therefore, encoding local environments is equivalent to one message passing layer, and its expressive power is a part of the expressive power of the whole GNN for PES. On the other hand, the interaction of two atoms will converge to zero if the distance approaches infinity. Therefore, the state of an atom is usually only closely related to the atoms close to it. Neglecting distant atoms and encoding local environments can capture the physical image better. Therefore, we study how well frames can be used to encode local environments.

The expressive power of encoding local environment reaches maximum when local environments can be mapped *injectively* to center atom representations. However, some popular models are under-expressive. For example, SchNet [Schütt et al., 2017] only considers the distance between atoms and neglects the angular information, leading to inability to differentiate some simple local environments as shown in Figure 2a. Moreover, Figure 2b illustrates that though DimeNet [Klicpera et al., 2020] adds angular information to message passing, its expressive power is still limited, which may be attributed to the loss of high-order geometric information like dihedral angles. In contrast, Proposition 4.3 shows that there exists a message passing scheme encoding local environments injectively with a local frame.

Proposition 4.3. *Given a frame \vec{E} , we can build a function ϕ as follows, which encodes local environments injectively, with suitable functions ρ and φ .*

$$\phi(\{(s_j, \vec{r}_{ij}) | r_{ij} < r_c\}) = \rho\left(\sum_{r_{ij} < r_c} \varphi(\text{Concatenate}(P_{\vec{E}}(\vec{r}_{ij}), s_j))\right). \quad (4)$$

Passing messages across local environments. Though an atom can only collect information from the local environment in one message passing step, messages can be passed across local environments along a path of atoms. However, most invariant models’ expressive power of multi-step message passing is still low. They lose the orientation information with only invariant messages passed across local environments. When a part of the molecule rotates, the center atom representations will be invariant, leading to the same energy prediction produced by them, while the true energy can change.

We can solve this problem by *frame-frame projection*, i.e., projecting the frame of atom j on the frame of atom i and adding the projection into the message from j to i . As shown in Figure 2c, frame-frame projection eliminates the information loss. A more formalized discussion is in Appendix G.

4.3 How to build a frame?

Usually, a frame should contain three linearly independent vectors. A straightforward idea is to use the atom feature, like kind of atom, to produce the frame. However, systems with central symmetry (like a single atom) cannot produce non-zero vectors as a frame. We formally characterize this phenomenon in the following proposition.

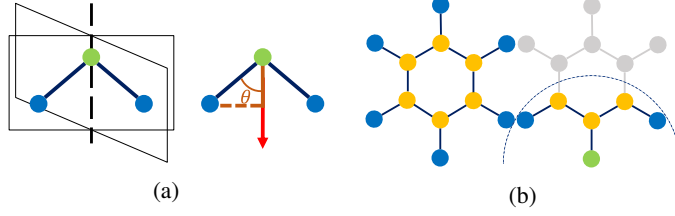


Figure 3: (a) The left part shows the symmetry of the water molecule in equilibrium, which has two planes of symmetry and a rotation axis. Its equivariant vectors must be parallel to the rotation axis. However, with a frame composed of only one vector, its geometry can be described. The right part shows that with the projection of \vec{r}_{ij} on the frame and the distance between two atoms, the angle θ and the position of j atom can be determined. (b) The left part is a molecule with central symmetry. All its vector features, including the global frame, will be zero. However, when selected as the center (green), the atom’s environment has no central symmetry.

Proposition 4.4. Assume that vector \vec{v} is a function of a set of atoms $\{(s_i, \vec{r}_i) | i = 1, 2, \dots\}$. If $\{(s_i, \vec{r}_i) | i = 1, 2, \dots\} = \{(s_i, -\vec{r}_i) | i = 1, 2, \dots\}$, then $\vec{v} = \vec{0}$.

Therefore, we consider producing the frame from the local environment of each atom. Intuitively, if an atom i has three non-symmetric neighbors not in the same plane, the neighbors’ relative positions \vec{r}_{ij} (sorted by their norm) can naturally build a frame for the center atom which is $O(3)$ -equivariant. However, for atoms with highly symmetric local environments, things can be different. Nevertheless, our main theorem shown below states that we can always find an $O(3)$ -equivariant frame for an atom from its local environment no matter how the local environment varies. Furthermore, the frame has full rank if the local environment has no symmetry.

Theorem 4.1. There exists an $O(3)$ -equivariant function g mapping the local environment LE_i to a frame $\vec{E}_i \in \mathbb{R}^{3 \times 3}$. The frame has full rank iff there does not exist $o \in O(3)$, $o \neq I$, $o(LE_i) = LE_i$.

Theorem 4.1 guarantees that we can always build a full-rank frame for an atom if its local environment has no symmetry.

In general, building a frame for symmetric molecules remains a problem but will not seriously hamper our model. Firstly, our model can produce reasonable output even with symmetric input and is provably more expressive than a widely used model SchNet [Schütt et al., 2017] (see Appendix J). Secondly, symmetric molecules are rare, which form a zero-measure set. In our two representative real-world datasets, less than 0.01% of molecules (about ten molecules in the whole datasets of several hundred thousand molecules) are symmetric. Thirdly, symmetric geometry may be captured with a degenerate frame. As shown in Figure 3a, water is a symmetric molecule. We can use a frame with one vector to describe its geometry. Last, a solution to frame degeneration is in Appendix K.

A message passing process for frame generation. There exists a universal framework for approximating $O(3)$ -equivariant functions [Villar et al., 2021] which can be used to implement the function g in Theorem 4.1. For scalability, we use a simplified form of that framework as follows.

$$\vec{E}_i = \sum_{j \neq i, r_{ij} < r_c} g'(r_{ij}, s_j) \circ \frac{\vec{r}_{ij}}{r_{ij}}, \quad (5)$$

where g' is some function mapping scalar features and distance to scalar weights and the entire framework reduces to a message passing process. The derivation is detailed in Appendix B.

Local frame vs global frame. With the message passing framework, a frame is produced for each atom. However, these local frames can also be summed to produce a global frame.

$$\vec{E} = \sum_{i=1}^n \vec{E}_i. \quad (6)$$

Global frame can replace local frame and keep the invariance of energy prediction. Moreover, if all atoms use the same frame, passing messages across local environments will be straightforward, as the frame-frame projection become trivial. However, the global frame is more likely to degenerate due to the symmetry of molecules. As shown in Figure 3b, the benzene molecule has central symmetry and

produces a zero global frame. However, when choosing each atom as the center, the central symmetry is broken and a meaningful local frame can be produced. We further formalize this intuition and prove that global frame is more likely to degenerate in Appendix L. We also discuss why we do not use the Gram-Schmidt process to make our frame vectors orthonormal in Appendix C.

5 GNN with local frame

Based on our previous analysis, we formally introduce our GNN with local frame (GNN-LF) model. The full architecture is detailed in Appendix D.

We first convert the input features of a molecule $\vec{r} \in \mathbb{R}^{N \times 3}$ and $z \in \mathbb{N}^N$ to a graph. The initial node feature $s_i^{(0)} \in \mathbb{R}^F$ is an embedding of the kind of atom z_i . For edge ij , we construct two features: the edge weight $w_{ij}^{(e)} = \text{cutoff}(r_{ij})$ (where cutoff means the cutoff function), and the radial basis expansion of the distance $s_{ij}^{(e)} = \text{rbf}(r_{ij})$. These special functions are detailed in Appendix D.

Scalar message function. The scalar message m_{ij} of edge ij is a function of the atom representations of i and j and the scalar features of edge ij . Concatenating them is enough to keep the expressive power. However, following Schütt et al. [2017], we use edge scalar features to produce a filter f_{ij} to filter the representation of atom j . Moreover, to make the message smooth to the cutoff ratio, edge weight $w_{ij}^{(e)}$ is used to scale the message. The message m_{ij} is computed as follows.

$$m_{ij} = w_{ij}^{(e)}(f_{ij} \odot s_j), \quad (7)$$

where \odot means element-wise product. Initially, $f_{ij} = f(s_{ij}^{(e)})$, where f is an invariant function outputting an F -dimensional scalar. This message function empirically works well, which may be attributed to its similarity to a quantum chemistry method [Tsubaki and Mizoguchi, 2020].

Producing frame. Combining Equation 5 and the form of scalar message in Equation 7, we get the form of the message passing scheme for producing the local frame (denoted by \vec{E}_i) as follows.

$$\vec{E}_i = \sum_{j \neq i, r_{ij} < r_c} w_{ij}^{(e)}(f_{ij} \odot s_j) \odot \frac{\vec{r}_{ij}}{r_{ij}}. \quad (8)$$

Note that $\vec{E}_i \in \mathbb{R}^{F \times 3}$ is not restricted to have three vectors, but grows with the embedding dimension F . This allows dimension consistency across the network and reduces the risk of degeneracy.

Projection of vector feature. With local frame, we can project the vector features on the frame and add them to the scalar edge features. For edge direction:

$$d_{ij}^1 = P(\frac{\vec{r}_{ij}}{r_{ij}}, \vec{E}_i), \quad d_{ij}^2 = P(\frac{\vec{r}_{ij}}{r_{ij}}, \vec{E}_j). \quad (9)$$

Note that d^1 is the edge direction projection on the center node, while d^2 is that on the neighbor node. Though d^1 is enough in our theoretical analysis, adding d^2 can bring a slight improvement in some of our experiments. Thus, we treat whether to use d^2 as a hyperparameter.

Directly using frame-frame projection leads to a large matrix. Therefore, we only use the diagonal elements of the projection. To keep the expressive power, we transform the frame with a linear layer before the inner product operation.

$$d_{ij}^3 = \langle W_1 \vec{v}_j, W_2 \vec{v}_i \rangle. \quad (10)$$

After all the projections, we update the filter function in (7) by including the additional scalars:

$$f_{ij} = f(s_{ij}^{(e)}, d_{ij}^1, d_{ij}^2, d_{ij}^3), \quad (11)$$

which is used in the later scalar message passing steps.

Decomposing filter. The filter function is further decomposed. The distance information is easier to learn as it has been expanded with a set of bases. Thus a linear layer g_1 is enough. In contrast, the directional information is the inner product of vectors, which may need a more expressive MLP g_2 . Therefore, we generate two filters separately.

$$f(s_{ij}^{(e)}, d_{ij}^1, d_{ij}^2, d_{ij}^3) = g_1(s_{ij}^{(e)}) \odot g_2(d_{ij}^1, d_{ij}^2, d_{ij}^3). \quad (12)$$

Table 1: Results on the MD17 dataset. Units: energy (E) (kcal/mol) and forces (F) (kcal/mol/Å).

		FCHL	SchNet	DimeNet	GemNet	PaiNN	NequIP	TorchMD	GNN-LF
Aspirin	E	0.182	0.37	0.204	-	0.167	-	0.124	<u>0.1342</u>
	F	0.478	1.35	0.499	<u>0.2168</u>	0.338	0.348	0.255	0.2018
Benzene	E	-	0.08	0.078	-	-	-	0.056	<u>0.0686</u>
	F	-	0.31	0.187	0.1453	-	0.187	0.201	<u>0.1506</u>
Ethanol	E	0.054	0.08	0.064	-	0.064	-	<u>0.054</u>	0.0522
	F	0.136	0.39	0.230	<u>0.0853</u>	0.224	0.208	0.116	0.0817
Malonaldehyde	E	0.081	0.13	0.104	-	0.091	-	<u>0.079</u>	0.0755
	F	0.245	0.66	0.383	<u>0.1545</u>	0.319	0.337	0.176	0.1239
Naphthalene	E	<u>0.117</u>	0.16	0.122	-	0.166	-	0.085	<u>0.1136</u>
	F	<u>0.151</u>	0.58	0.215	<u>0.0553</u>	0.077	0.097	0.060	0.0550
Salicylic acid	E	0.114	0.20	0.134	-	0.166	-	0.094	<u>0.1074</u>
	F	0.221	0.85	0.374	<u>0.1268</u>	0.195	0.238	0.135	0.1005
Toluence	E	0.098	0.12	0.102	-	0.095	-	0.074	<u>0.0950</u>
	F	0.203	0.57	0.216	<u>0.0600</u>	0.094	0.101	0.066	0.0529
Uracil	E	0.104	0.14	0.115	-	0.106	-	0.096	<u>0.1037</u>
	F	0.105	0.56	0.301	0.0969	0.139	0.173	<u>0.094</u>	0.0751
average	rank	3.93	6.63	5.38	2.00	4.36	5.25	2.25	1.75

Sharing filters. Generating different filters for each message passing layer is time-consuming, as $O(Nn)$ filters need to be computed in each layer. Therefore, we share filters between different layers. Experimental results show that sharing filters only leads to minor performance loss.

6 Experiment

In this section, we compare GNN-LF with existing models on different tasks and do ablation analysis. We report the mean absolute error (MAE) on test set (the lower the better) for all tasks. All our results are averaged over three random dataset splits. Baselines’ results are from their original papers. The best results are shown in bold and the second best results are shown with underlines in tables. Our experimental settings are detailed in Appendix E.

6.1 Modeling PES

We first evaluate our models for modeling PES on the MD17 dataset [Chmiela et al., 2017], which consists of MD trajectories of small organic molecules. We compare our model with a manual descriptor model: FCHL [Christensen et al., 2020], invariant models: SchNet [Schütt et al., 2017], DimeNet [Klicpera et al., 2020], GemNet [Gasteiger et al., 2021], a model using irreducible representations of $SO(3)$ group: NequIP [Batzner et al., 2021], and models using vector representations: PaiNN [Schütt et al., 2021] and TorchMD [Thölke and Fabritiis, 2022]. The results are shown in Table 1. Our model outperforms all the baselines on **nine out of sixteen targets** and achieves the second-best performance on **all other seven targets**, which is better than any other model. Compared with GemNet, the model with the second highest average rank, our model leads to 10% lower loss on average. The outstanding performance verifies the effectiveness of the local frame method for modeling PES. Moreover, our model also uses fewer parameters and **less than 30% computation time** compared with the baselines as shown in Appendix F.

6.2 Ablation study

We perform an ablation study to verify our model designs. The results are shown in Table 2. On average, ablation of d^3 term in Equation (10) (NoDir3) leads to 20% higher MAE, which verifies the necessity of frame-frame projection. In contrast, ablation of the d^2 term in Equation (9) (NoDir2) only results in 1% higher MAE on three datasets, which illustrates that, as shown in our theoretical analysis, projection of direction on the target node and frame is enough for high expressive power. The column Global replaces the local frames with the pooled global frame, resulting in 100% higher loss, which verifies the advantages of local frames. Ablation of filter decomposition (NoDecomp) leads to 9% higher loss, indicating the advantage of separately processing distance and projections. Finally, we find although using different filters for each message passing layer (NoShare) uses much

Table 2: Ablation results on the MD17 dataset. Units: energy (E) (kcal/mol) and forces (F) (kcal/mol/Å). GNN-LF does not use d^2 for some molecules, so the NoDir2 column is empty.

		GNN-LF	NoDir2	NoDir3	Global	NoDecomp	GNN-LF	Noshare
Aspirin	E	0.1342	-	0.1435	0.2280	0.1411	0.1342	0.1364
	F	0.2018	-	0.2799	0.6894	0.2622	0.2018	0.1979
Benzene	E	0.0686	-	0.0716	0.0972	0.0688	0.0686	0.0713
	F	0.1506	-	0.1583	0.3520	0.1499	0.1506	0.1507
Ethanol	E	0.0520	-	0.0532	0.0556	0.0518	0.0520	0.0514
	F	0.0814	-	0.0930	0.1465	0.0847	0.0814	0.0751
Malonaldehyde	E	0.0755	0.0764	0.0776	0.0923	0.0762	0.0755	0.0790
	F	0.1239	0.1259	0.1466	0.3194	0.1321	0.1239	0.1210
Naphthalene	E	0.1136	-	0.1152	0.1276	0.1254	0.1136	0.1168
	F	0.0550	-	0.0834	0.2069	0.0553	0.0550	0.0547
Salicylic acid	E	0.1074	0.1081	0.1087	0.1224	0.1123	0.1074	0.1091
	F	0.1005	0.1048	0.1328	0.2890	0.1399	0.1005	0.1012
Toluence	E	0.0950	0.0930	0.0942	0.1000	0.0932	0.0950	0.0942
	F	0.0529	0.0543	0.0770	0.1659	0.0695	0.0529	0.0519
Uracil	E	0.1037	-	0.1069	0.1075	0.1053	0.1037	0.1042
	F	0.0751	-	0.0964	0.1901	0.0825	0.0751	0.0754

Table 3: Results on the QM9 dataset.

Target	Unit	SchNet	DimeNet++	Cormorant	PaiNN	Torchmd	GNN-LF
μ	D	0.033	0.0297	0.038	0.012	0.002	0.013
α	a_0^3	0.235	0.0435	0.085	0.045	0.01	<u>0.0353</u>
ϵ_{HOMO}	meV	41	24.6	34	27.6	21.2	<u>23.5</u>
ϵ_{LUMO}	meV	34	19.5	38	20.4	<u>17.8</u>	17.0
$\Delta\epsilon$	meV	63	32.6	61	45.7	38	<u>37.1</u>
$\langle R^2 \rangle$	a_0^2	0.073	0.331	0.961	0.066	0.015	<u>0.037</u>
ZPVE	meV	1.7	<u>1.21</u>	2.027	1.28	2.12	1.19
U_0	meV	14	6.32	22	<u>5.85</u>	6.24	5.30
U	meV	19	6.28	21	<u>5.83</u>	6.30	5.24
H	meV	14	6.53	21	<u>5.98</u>	6.48	5.48
G	meV	14	7.56	20	<u>7.35</u>	7.64	6.84
C_v	cal/mol/K	0.033	<u>0.023</u>	0.026	0.024	0.026	0.022

more computation time ($1.67\times$) and parameters ($3.55\times$), it only leads to 0.01% lower loss on average, illustrating that sharing filters does little harm to the expressive power.

6.3 Other chemical properties

Though designed for PES, our model can also predict other properties directly. The QM9 dataset [Wu et al., 2018] consists of 134k stable small organic molecules. The task is to use the kind of atoms z and coordinates of atoms \vec{r} to predict 12 properties of these molecules. We compare our model with invariant models: SchNet [Schütt et al., 2017], DimeNet++ [Gasteiger et al., 2020], a model using irreducible representations: Cormorant [Anderson et al., 2019], and models using vector representations: PaiNN [Schütt et al., 2021] and TorchMD [Thölke and Fabritiis, 2022]. The results are shown in Table 3. Our model outperforms all other models on seven out of twelve tasks and achieves the second-best performance on four out of the five left tasks, which illustrates that the local frame method has the potential to be applied to other fields.

7 Conclusion

This paper proposes a local frame method, which avoids passing vector representations during message passing while keeping high expressive power. We show that local frames enable GNNs to encode local environments around atoms injectively and pass orientation information across local environments. Furthermore, we give conditions for the existence of local frames and propose ways to construct them. In the experiments, our model outperforms all baselines on modeling PES and predicting other properties, while using fewer parameters and less inference time, which verifies the simplicity, effectiveness and scalability of the local frame method.

References

- Gunnar Schmitz, Ian Heide Godtlielsen, and Ove Christiansen. Machine learning for potential energy surfaces: An extensive database and assessment of methods. *The Journal of Chemical Physics*, 150(24):244113, 2019.
- Errol G. Lewars. *The Concept of the Potential Energy Surface*, pages 9–49. Springer International Publishing, 2016.
- K. T. Schutt, F. Arbabzadah, S. Chmiela, K.-R. Muller, and A. Tkatchenko. Quantum-chemical insights from deep tensor neural networks. *Nature Communications*, 8:13890, 2017.
- Kristof Schütt, Pieter-Jan Kindermans, Huziel Enoc Saucedo Felix, Stefan Chmiela, Alexandre Tkatchenko, and Klaus-Robert Müller. Schnet: A continuous-filter convolutional neural network for modeling quantum interactions. In *Advances in Neural Information Processing Systems 30*, pages 991–1001, 2017.
- Johannes Klicpera, Janek Groß, and Stephan Günnemann. Directional message passing for molecular graphs. In *International Conference on Learning Representations*, 2020.
- Brandon M. Anderson, Truong-Son Hy, and Risi Kondor. Cormorant: Covariant molecular neural networks. In *Advances in Neural Information Processing Systems*, pages 14510–14519, 2019.
- Kristof Schütt, Oliver T. Unke, and Michael Gastegger. Equivariant message passing for the prediction of tensorial properties and molecular spectra. In *International Conference on Machine Learning*, volume 139, pages 9377–9388, 2021.
- Johannes Gasteiger, Florian Becker, and Stephan Günnemann. Gemnet: Universal directional graph neural networks for molecules. In *Advances in Neural Information Processing Systems*, 2021.
- Simon L. Batzner, Tess E. Smidt, Lixin Sun, Jonathan P. Mailoa, Mordechai Kornbluth, Nicola Molinari, and Boris Kozinsky. Se(3)-equivariant graph neural networks for data-efficient and accurate interatomic potentials. *CoRR*, abs/2101.03164, 2021.
- Philipp Thölke and Gianni De Fabritiis. Equivariant transformers for neural network based molecular potentials. In *International Conference on Learning Representations*, 2022.
- Thomas N. Kipf and Max Welling. Semi-supervised classification with graph convolutional networks. *International Conference on Learning Representations*, 2017.
- Nathaniel Thomas, Tess E. Smidt, Steven Kearnes, Lusann Yang, Li Li, Kai Kohlhoff, and Patrick Riley. Tensor field networks: Rotation- and translation-equivariant neural networks for 3d point clouds. *CoRR*, abs/1802.08219, 2018.
- Matthias Rupp, Alexandre Tkatchenko, Klaus-Robert Müller, and O. Anatole von Lilienfeld. Fast and accurate modeling of molecular atomization energies with machine learning. *Physical Review Letter*, 108:058301, Jan 2012.
- Stefan Chmiela, Huziel E. Saucedo, Igor Poltavsky, Klaus-Robert Müller, and Alexandre Tkatchenko. sgdm: Constructing accurate and data efficient molecular force fields using machine learning. *Computer Physics Communications*, 240:38–45, 2019.
- Anders S Christensen, Lars A Bratholm, Felix A Faber, and O Anatole von Lilienfeld. Fchl revisited: Faster and more accurate quantum machine learning. *The Journal of chemical physics*, 152(4): 044107, 2020.
- Jörg Behler and Michele Parrinello. Generalized neural-network representation of high-dimensional potential-energy surfaces. *Physical Review Letter*, 98:146401, 2007.
- J. S. Smith, O. Isayev, and A. E. Roitberg. Ani-1: an extensible neural network potential with dft accuracy at force field computational cost. *Chem. Sci.*, 8:3192–3203, 2017.
- Linfeng Zhang, Jiequn Han, Han Wang, Wissam Saidi, Roberto Car, and Weinan E. End-to-end symmetry preserving inter-atomic potential energy model for finite and extended systems. In *Advances in Neural Information Processing Systems*, 2018.

- Weitao Du, He Zhang, Yuanqi Du, Qi Meng, Wei Chen, Nanning Zheng, Bin Shao, and Tie-Yan Liu. SE(3) equivariant graph neural networks with complete local frames. In Kamalika Chaudhuri, Stefanie Jegelka, Le Song, Csaba Szepesvári, Gang Niu, and Sivan Sabato, editors, *International Conference on Machine Learning*, 2022.
- Victor Garcia Satorras, Emiel Hoogetboom, and Max Welling. E(n) equivariant graph neural networks. In *International Conference on Machine Learning*, 2021.
- Shitong Luo, Jiahao Li, Jiaqi Guan, Yufeng Su, Chaoran Cheng, Jian Peng, and Jianzhu Ma. Equivariant point cloud analysis via learning orientations for message passing. In *IEEE Conference on Computer Vision and Pattern Recognition*, pages 16296–16305, 2021.
- Wenbing Huang, Jiaqi Han, Yu Rong, Tingyang Xu, Fuchun Sun, and Junzhou Huang. Equivariant graph mechanics networks with constraints. *International Conference on Learning Representations*, 2022.
- Soledad Villar, David W Hogg, Kate Storey-Fisher, Weichi Yao, and Ben Blum-Smith. Scalars are universal: Equivariant machine learning, structured like classical physics. In *Advances in Neural Information Processing Systems*, 2021.
- Congyue Deng, Or Litany, Yueqi Duan, Adrien Poulenard, Andrea Tagliasacchi, and Leonidas J. Guibas. Vector neurons: A general framework for so(3)-equivariant networks. In *International Conference on Computer Vision*, pages 12180–12189. IEEE, 2021.
- Masashi Tsubaki and Teruyasu Mizoguchi. On the equivalence of molecular graph convolution and molecular wave function with poor basis set. In H. Larochelle, M. Ranzato, R. Hadsell, M.F. Balcan, and H. Lin, editors, *Advances in Neural Information Processing Systems*, volume 33, pages 1982–1993. Curran Associates, Inc., 2020.
- Stefan Chmiela, Alexandre Tkatchenko, Huziel E. Sauceda, Igor Poltavsky, Kristof T. Schütt, and Klaus-Robert Müller. Machine learning of accurate energy-conserving molecular force fields. *Science Advances*, 3(5):e1603015, 2017.
- Zhenqin Wu, Bharath Ramsundar, Evan N. Feinberg, Joseph Gomes, Caleb Geniesse, Aneesh S. Pappu, Karl Leswing, and Vijay Pande. Moleculenet: a benchmark for molecular machine learning. *Chemical Science*, 9:513–530, 2018.
- Johannes Gasteiger, Shankari Giri, Johannes T. Margraf, and Stephan Günnemann. Fast and uncertainty-aware directional message passing for non-equilibrium molecules. In *Machine Learning for Molecules Workshop, NeurIPS*, 2020.
- Manzil Zaheer, Satwik Kottur, Siamak Ravanbakhsh, Barnabás Póczos, Ruslan Salakhutdinov, and Alexander J. Smola. Deep sets. In *Advances in Neural Information Processing Systems*, pages 3391–3401, 2017.
- Viktoriia Kravtsov and Andriy Zagorodnyuk. On algebraic bases of algebras of block-symmetric polynomials on banach spaces. *Matematychni Studii*, 37, 03 2012.
- Oliver Unke and Markus Meuwly. Physnet: A neural network for predicting energies, forces, dipole moments and partial charges. *J Chem Theory Comput.*, 6:3678–3693, 02 2019.
- Nimrod Segol and Yaron Lipman. On universal equivariant set networks. In *International Conference on Learning Representations*, 2020.
- Nadav Dym and Haggai Maron. On the universality of rotation equivariant point cloud networks. In *International Conference on Learning Representations*, 2021.
- Omri Puny, Matan Atzmon, Heli Ben-Hamu, Edward J. Smith, Ishan Misra, Aditya Grover, and Yaron Lipman. Frame averaging for invariant and equivariant network design. *International Conference on Learning Representations*, 2022.

Checklist

The checklist follows the references. Please read the checklist guidelines carefully for information on how to answer these questions. For each question, change the default **[TODO]** to **[Yes]**, **[No]**, or **[N/A]**. You are strongly encouraged to include a **justification to your answer**, either by referencing the appropriate section of your paper or providing a brief inline description. For example:

- Did you include the license to the code and datasets? **[No]** The code and the data are proprietary.

1. For all authors...

- (a) Do the main claims made in the abstract and introduction accurately reflect the paper's contributions and scope? **[Yes]**
- (b) Did you describe the limitations of your work? **[Yes]**
- (c) Did you discuss any potential negative societal impacts of your work? **[N/A]**
- (d) Have you read the ethics review guidelines and ensured that your paper conforms to them? **[Yes]**

2. If you are including theoretical results...

- (a) Did you state the full set of assumptions of all theoretical results? **[Yes]**
- (b) Did you include complete proofs of all theoretical results? **[Yes]**

3. If you ran experiments...

- (a) Did you include the code, data, and instructions needed to reproduce the main experimental results (either in the supplemental material or as a URL)? **[Yes]**
- (b) Did you specify all the training details (e.g., data splits, hyperparameters, how they were chosen)? **[Yes]**
- (c) Did you report error bars (e.g., with respect to the random seed after running experiments multiple times)? **[No]** Existing works seldom report error bars.
- (d) Did you include the total amount of compute and the type of resources used (e.g., type of GPUs, internal cluster, or cloud provider)? **[Yes]** We use internal cluster and clarify our GPU resource.

4. If you are using existing assets (e.g., code, data, models) or curating/releasing new assets...

- (a) If your work uses existing assets, did you cite the creators? **[Yes]**
- (b) Did you mention the license of the assets? **[Yes]**
- (c) Did you include any new assets either in the supplemental material or as a URL? **[No]**
- (d) Did you discuss whether and how consent was obtained from people whose data you're using/curating? **[N/A]**
- (e) Did you discuss whether the data you are using/curating contains personally identifiable information or offensive content? **[N/A]**

5. If you used crowdsourcing or conducted research with human subjects...

- (a) Did you include the full text of instructions given to participants and screenshots, if applicable? **[N/A]**
- (b) Did you describe any potential participant risks, with links to Institutional Review Board (IRB) approvals, if applicable? **[N/A]**
- (c) Did you include the estimated hourly wage paid to participants and the total amount spent on participant compensation? **[N/A]**

A Proofs

Due to repulsive force, atoms cannot be too close to each other in stable molecules. Therefore, we assume that there exist an upper bound N of the number of neighbor atoms.

A.1 Proof of Lemma 3.1

Proof. For all function g , scalar s , transformation $o \in \text{O}(3)$, $g(s(z, \vec{r}o^T)) = g(s)$. Therefore, $g(s)$ is a scalar.

For all scalar s , vector \vec{v} , and transformation $o \in \text{O}(3)$, $s(z, \vec{r}o^T) \circ \vec{v}(z, \vec{r}o^T) = s(z, \vec{r}) \circ (\vec{v}(z, \vec{r})o^T) = (s(z, \vec{r}) \circ \vec{v}(z, \vec{r}))o^T$. Therefore, $s \circ \vec{v}$ is a vector.

For all vectors \vec{v}_1, \vec{v}_2 , $\vec{v}_1(z, \vec{r}o^T)\vec{v}_2(z, \vec{r}o^T)^T = \vec{v}_1(z, \vec{r})o^T o\vec{v}_2(z, \vec{r})^T = \vec{v}_1(z, \vec{r})\vec{v}_2(z, \vec{r})^T$.

As $P(\vec{v}_1, \vec{v}_2)$ is a scalar, $\langle \vec{v}_1, \vec{v}_2 \rangle = \text{diag}(P(\vec{v}_1, \vec{v}_2))$ must be a scalar. \square

A.2 Proof of Proposition 4.1

Proof. Let \vec{v} denote a vector. $P_{\vec{E}}(\vec{v})$ is scalar because

$$\forall o \in \text{O}(3), P_{\vec{E}}(\vec{v})(z, \vec{r}o^T) = \vec{v}(z, \vec{r}o^T)\vec{E}(z, \vec{r}o^T)^T \quad (13)$$

$$= \vec{v}(z, \vec{r})o^T o\vec{E}(z, \vec{r})^T \quad (14)$$

$$= P_{\vec{E}}(\vec{v})(z, \vec{r}). \quad (15)$$

$P_{\vec{E}}$ is bijective as $\vec{x} = P_{\vec{E}}(\vec{x})(\vec{E}^{-1})^T$. Obviously, $P_{\vec{E}}^{-1}(s) = s(\vec{E}^{-1})^T$, $s \in \mathbb{R}^{F \times 3}$, s is a scalar representation. To prove that $P^{-1}(s)$ is a vector representation, we note that $P^{-1}(s)$ is itself a function of (z, \vec{r}) , which can be written as $P^{-1}(s)(z, \vec{r})$. We have

$$\forall o \in \text{O}(3), P_{\vec{E}}^{-1}(s)(z, \vec{r})o^T = s(z, \vec{r})[(\vec{E}(z, \vec{r})o^T)^{-1}]^T \quad (16)$$

$$= s(z, \vec{r}o^T)(\vec{E}(z, \vec{r}o^T)^{-1})^T \quad (17)$$

$$= P_{\vec{E}}^{-1}(s)(z, \vec{r}o^T). \quad (18)$$

Therefore, $P_{\vec{E}}^{-1}(s)$ is a vector representation. \square

A.3 Proof of Proposition 4.2

Proof. Assume that s is a scalar representation.

$$\tilde{g}(s) = P_{\vec{E}}(g(P_{\vec{E}}^{-1}(s))) \quad (19)$$

$$= g(s(\vec{E}(z, \vec{r})^{-1})^T)\vec{E}(z, \vec{r})^T. \quad (20)$$

The representation $\tilde{g}(s)$ can be written as a function of (z, \vec{r}) . Then, we have

$$\forall o \in \text{O}(3), \tilde{g}(s)(z, \vec{r}o^T) = g(s(\vec{E}(z, \vec{r}o^T)^{-1})^T)\vec{E}(z, \vec{r}o^T)^T \quad (21)$$

$$= g(s(\vec{E}(z, \vec{r})^{-1})^T)o^T o\vec{E}(z, \vec{r})^T \quad (22)$$

$$= g(s(\vec{E}(z, \vec{r})^{-1})^T)o^T o\vec{E}(z, \vec{r})^T \quad (23)$$

$$= g(s(\vec{E}(z, \vec{r})^{-1})^T)\vec{E}(z, \vec{r})^T \quad (24)$$

$$= \tilde{g}(s)(z, \vec{r}). \quad (25)$$

Therefore, $\tilde{g}(s)$ is also a scalar representation. \square

A.4 Proof of Proposition 4.3

Let γ denote a function mapping local environments to a set of scalars with a frame.

$$\gamma(\{(s_j, \vec{r}_{ij}) | r_{ij} < r_c\}) = \{\text{Concatenate}(s_j, P_{\vec{E}}(\vec{r}_{ij})) | r_{ij} < r_c\}. \quad (26)$$

As it has an inverse function, γ is injective.

$$\gamma^{-1}(\{s_j | j = 1, 2, \dots\}) = \{(s_j[-3], P_E^{-1}(s_j[-3 :])|j = 1, 2, \dots)\}. \quad (27)$$

Therefore, we only need an expressive scalar aggregation function. Zaheer et al. [2017] proved the existence of such function for scalar in $[0, 1]$. However, our scalar feature $\in \mathbb{R}^F$, where F is a hyperparameter usually ≥ 4 , so we extend the conclusion of Zaheer et al. [2017].

Lemma A.1. *There exists a function ψ mapping a scalar set of size $\leq N$ to a scalar injectively.*

Proof. For a set of scalar $S = \{s_i | i = 1, 2, \dots, n, s^{(i)} \in \mathbb{R}^F\}$, we define a polynomial as follows.

$$p^{(S)}(x_1, \dots, x_F) = \prod_{i=1}^n [\sum_{j=1}^F (x_i - s_{ij})^2], \quad (28)$$

where s_{ij} is the j^{th} element of s_i . $p^{(S)}(x_1, \dots, x_F)$ is a $2nF$ -order polynomial. Let C_t donate the coefficient of the t -th term by some order. C_t is a polynomial of $s_j^{(i)}$, $i = 1, 2, \dots, n, j = 1, 2, \dots, F$ and can be formalized as follows.

$$C_t = \sum_D \alpha^{(t,D)} \prod_{i=1}^n \prod_{j=1}^F s_{ij}^{d_{ij}}, \quad (29)$$

where $D \in \{[d_{11}, d_{12}, \dots, d_{ij}, \dots, d_{nF}] | d_{ij} \in \mathbb{N}, \sum_{ij} d_{ij} \leq 2nF\}$. Note that C_t is symmetric to the permutation of i . Such polynomials are called *block-symmetric polynomial* [Kravtsiv and Zagorodnyuk, 2012].

As shown in [Kravtsiv and Zagorodnyuk, 2012], the generating elements of block-symmetric polynomial are as follows.

$$H_{\kappa}^{k_1, k_2, \dots, k_F} = \sum_{i=1}^n \prod_{j=1}^F s_{ij}^{k_i}, \sum_{j=1}^F k_j = \kappa. \quad (30)$$

Because degree of C_t is less than $2nF + 1$, C_t is a function of $[H_{\kappa}^{k_1, k_2, \dots, k_F} | \sum_{j=1}^F k_j = \kappa, \kappa = 1, 2, \dots, 2nF]$.

Let $\varphi(s_i) = [\prod_{j=1}^F s_{ij}^{k_j} | \sum_{j=1}^F k_j = \kappa, \kappa = 1, 2, \dots, 2nF]$. $\sum_i \varphi(s_i) = [H_{\kappa}^{k_1, k_2, \dots, k_F} | \sum_{j=1}^F k_j = \kappa, \kappa = 1, 2, \dots, 2nF]$ determines C_t and the polynomial $p^{(S)}(x_1, \dots, x_F)$.

Assuming that $S \neq S'$ but $\sum_i \varphi(s_i) = \sum_i \varphi(s'_i)$. Therefore, $p^{(S)}(x_1, \dots, x_F) = p^{(S')}(x_1, \dots, x_F)$. Therefore, for all $s_i \in S$, $p^{(S')}(s_{i1}, s_{i2}, \dots, s_{iF}) = p^{(S)}(s_{i1}, s_{i2}, \dots, s_{iF}) = 0$, $s \in S'$. Therefore, $S \subseteq S'$. As $|S| = |S'| = n$, $S = S'$, leading to a contradiction.

Therefore, given two set of scalars $S = \{s_i | s_i \in \mathbb{R}^F, i = 1, 2, \dots, n\}$, $S' = \{s'_i | s'_i \in \mathbb{R}^F, i = 1, 2, \dots, n\}$, $S \neq S' \iff \sum_i \varphi(s_i) \neq \sum_i \varphi(s'_i)$. There also exists a function ψ_n map sets of n elements from \mathbb{R}^F injectively.

$$\psi_n(\{s_i | s_i \in \mathbb{R}^F, i = 1, 2, \dots, n\}) = \rho_n(\sum_{i=1}^n \phi_n(x_i)), \quad (31)$$

where ρ_n, ϕ_n are suitable functions.

Let $\phi(s)$ denote the sequence $[1, \phi_0(s), \dots, \phi_N(s)]$. Therefore $\sum_{i=1}^n \phi(s_i)$ is a sequence $[n, \sum_{i=1}^n \phi_0(s_i), \dots, \sum_{i=1}^n \phi_N(s_i)]$. Let $\rho(n, \sum_{i=1}^n \phi_0(s_i), \dots, \sum_{i=1}^n \phi_N(s_i))$ produce a output pair $[n, \rho_n(\sum_{i=1}^n \phi_n(s_i))]$. Let $\psi(S) = \tilde{\rho}(\sum_{s \in S} \phi(s))$. Therefore, ψ can map feature sets of size $\leq N$ injectively. \square

A.5 Proof of Proposition 4.4

$$\vec{v}(\{(s_i, -\vec{r}_i)\}) = \vec{v}(\{(s_i, \vec{r}_i \begin{bmatrix} -1 & 0 & 0 \\ 0 & -1 & 0 \\ 0 & 0 & -1 \end{bmatrix})\}) \quad (32)$$

$$= \vec{v}(\{(s_i, \vec{r}_i)\}) \begin{bmatrix} -1 & 0 & 0 \\ 0 & -1 & 0 \\ 0 & 0 & -1 \end{bmatrix} \quad (33)$$

$$= -\vec{v}(\{(s_i, \vec{r}_i)\}). \quad (34)$$

Therefore, if $\{(s_i, \vec{r}_i)\} = \{(s_i, -\vec{r}_i)\}$, $\vec{v}(\{(s_i, \vec{r}_i)\}) = -\vec{v}(\{(s_i, \vec{r}_i)\}) = 0$.

A.6 Proof of Theorem 4.1

Proof. (1) We first prove there exists an $O(3)$ -equivariant function g mapping the local environment LE_i to a frame $\vec{E}_i \in \mathbb{R}^{3 \times 3}$. The frame has full rank if there does not exist $o \in O(3)$, $o \neq I$, $o(LE_i) = LE_i$.

Let γ denote a function mapping local environments to sets of vectors.

$$\gamma(\{(\vec{r}_{ij}, s_j) | r_{ij} < r_c\}) = \{\text{Concatenate}(s_j \vec{r}_{ij}, \vec{r}_{ij}) | r_{ij} < r_c\}, \quad (35)$$

in which s_j is reshaped as $(F, 1)$, \vec{r}_{ij} is of shape $(1, 3)$. γ is $O(3)$ -equivariant. Therefore, we discuss the aggregation function on a set of vector, denoted as $\{\vec{u}_i | i = 1, 2, \dots, n, \vec{u}_i \in \mathbb{R}^{F \times 3}\}$.

Assume that $V = \{\{\vec{u}_i | i = 1, 2, \dots, n, \vec{u}_i \in \mathbb{R}^{F \times 3}\} | n = 1, 2, \dots, N\}$, where N is the upper bound of the size of local environment, is the set of sets of vector messages in local environment.

An equivalence relation can be defined on V : $v_1 \in V, v_2 \in V, v_1 \sim v_2$ iff there exists $o \in O(3)$, $o(v_1) = v_2$. Let $\tilde{V} = V / \sim$ denote the quotient set. For each equivalence class $[v]$ with no symmetry, a representative v can be selected. We can define a function $r : \tilde{V} - \{[v] | [v] \in \tilde{V}, \exists v \in [v], o \in O(3), o \neq I, o(v) = v\} \rightarrow V$ as $r([v]) = v$ mapping each equivalence class with no symmetry to its representative. For a message set with no symmetry, the transformation from its representative to it is also unique. Let $h : V - \{v | v \in V, \exists o \in O(3), o \neq I, o(v) = v\} \rightarrow O(3)$. $h(v) = o, o(r([v])) = v$.

Therefore, the function g can take the form as follows.

$$g(v) = \begin{cases} \begin{bmatrix} 0 & 0 & 0 \\ 0 & 0 & 0 \\ 0 & 0 & 0 \end{bmatrix} & \text{if there exists } o \in O(3), o \neq I, ov = v \\ h(v)^T & \text{otherwise} \end{cases}$$

Therefore, $g \cdot \gamma$ is the required function.

We further detail how to select the representative elements: We first define a linear order relation \leq_l in V . If $v_1, v_2 \in V, |v_1| < |v_2|, v_1 <_l v_2$. So we only consider the order relation between two sets of the same size n .

We first define a function ψ mapping message set to a sequence injectively.

$$\psi(\{u_i | i = 1, 2, \dots, n, u_i \in \mathbb{R}^{F \times 3}\}) = [\text{flatten}(u_{\pi(i)}) | i = 1, 2, \dots, n, \pi \text{ is a permutation sorting } u_i \text{ by lexicographical order}]. \quad (36)$$

For all $v_1, v_2 \in V, |v_1| = |v_2|, v_1 \leq_l v_2$ iff $\psi(v_1) \leq \psi(v_2)$ by lexicographical order. As the size of local environment is bounded, the sequence is also of a finite length. Therefore, the lexicographical order and thus the linear order relation \leq_l are well-defined.

All permutations of $\{1, 2, \dots, n\}$ form a permutation set Π_n .

For all $[v] \in \tilde{V}$, let $r([v]) = \arg \min_{v' \in [v]} \psi(v')$. To illustrate the existence of such minimal sequence, we reform it.

$$\min_{v' \in [v]} \psi(v') = \min_{\pi \in \Pi_n, o \in O(3)} S(o, \pi) \quad (37)$$

$$= \min_{\pi \in \Pi_n} \min_{o \in O(3)} S(o, \pi), \quad (38)$$

where $S(o, \pi) = [\text{flatten}(u_{\pi(i)} o^T)]_{i=1, 2, \dots, n}$. Each element of this sequence is continuous to o .

We first fix the π . As $O(3)$ is a compact group, $\arg \min_{o \in O(3)} S(o, \pi)_1$ exists. Let $L_1 = \{o | o \in O(3), S(o, \pi)_1 = \min_{o' \in O(3)} S(o', \pi)_1\}$ is still a compact set. Therefore, $\arg \min_{o \in L_1} S(o, \pi)_1$ exists. Let $L_2 = \{o | o \in L_1, S(o, \pi)_2 = \min_{o' \in L_1} S(o', \pi)_2\}$. Similarly, L_3, L_4, \dots, L_{3Fn} can be defined and they are non-empty set. For all $o_1, o_2 \in L_{3Fn}$, as $S(o_1, \pi) \leq S(o_2, \pi)$ and $S(o_2, \pi) \leq S(o_1, \pi)$ by lexicographical order, $S(o_2, \pi) = S(o_1, \pi)$ and thus $o_1(v) = o_2(v)$. If v has no symmetry, $\forall o \in O(3), o \neq I, o(v) \neq v, o_1(v) = o_2(v) \implies o_1 = o_2$. Therefore, L_{3Fn} contains a unique element $o_v^{(0)}$ and $\min_{o \in O(3)} S(o, \pi)$ is unique.

As Π_n is a finite set, if $\min_{o \in O(3)} S(o, \pi)$ exist for all $\pi \in \Pi_n$, $\min_{\pi \in \Pi_n} \min_{o \in O(3)} S(o, \pi)$ must exist. Therefore the minimal sequence exists. As \leq_l is a linear order, the minimal sequence is unique. With the unique sequence, the unique representative can be determined.

(2) Then we prove there does not exist $o \in O(3), o \neq I, o(LE_i) = LE_i$ if the frame has full rank.

The frame \vec{E} is a function of local environment. If there exists

$$o \in O(3), o(LE_i) = LE_i.$$

Then $\vec{E}(o(LE_i)) = \vec{E}(LE_i) o^T = \vec{E}(LE_i)$.

As \vec{E} is a invertible matrix, $o = I$. Therefore, LE_i has no symmetry.

□

B Derivation of the message passing section for frame

The framework proposed by Villar et al. [2021] is

$$h_n(\{\vec{m}_{i1}, \vec{m}_{i2}, \vec{m}_{i3}, \dots, \vec{m}_{in}\}) = \sum_{j=1}^n g(\vec{m}_{ij}, \{\vec{m}_{i1}, \dots, \vec{m}_{in}\} - \{\vec{m}_{ij}\}) \circ \vec{m}_{ij}, \quad (39)$$

where h_n is the aggregation function for n messages. g is a $O(3)$ -invariant functions. We can further reform it.

$$h_n(\{\{\vec{m}_{i1}, \vec{m}_{i2}, \dots, \vec{m}_{in}\}\}) = \sum_{j=1}^n g_1^{(n)}(g_2^{(n)}(\vec{m}_{ij}), h_{n-1}(\{\vec{m}_{i1}, \vec{m}_{i2}, \dots, \vec{m}_{in}\} - \{\vec{m}_{ij}\})) \vec{m}_{ij}, \quad (40)$$

where $g_1^{(n)}, g_2^{(n-1)}$ are two $O(3)$ -invariant functions. With this equation, we can recursively build n messages aggregation function h_n with h_{n-1} . Its universal approximation power has been proved in [Villar et al., 2021].

However, as they can have varied numbers of neighbors, different nodes have to use different aggregation functions, which is hard to implement. Therefore, we assume that the aggregation function keeps the same form for different sizes of the message multiset and desert the recursive term h_{n-1} .

$$h_n(\{\{\vec{m}_{i1}, \vec{m}_{i2}, \dots, \vec{m}_{in}\}\}) = \sum_{j=1}^n g(\vec{m}_{ij}) \vec{m}_{ij}. \quad (41)$$

The message \vec{m}_{ij} can have the form $\text{Concatenate}(1, s) \circ \vec{r}_{ij}$ in Proposition 4.1. As g is a invariant function, we can further simplify Equation 41.

$$h_n(\{\{\vec{m}_{i1}, \vec{m}_{i2}, \dots, \vec{m}_{in}\}\}) = \sum_{j=1}^n g'(r_{ij}, s_j) \frac{\vec{r}_{ij}}{r_{ij}}, \quad (42)$$

where g' is a function mapping scalars to scalars.

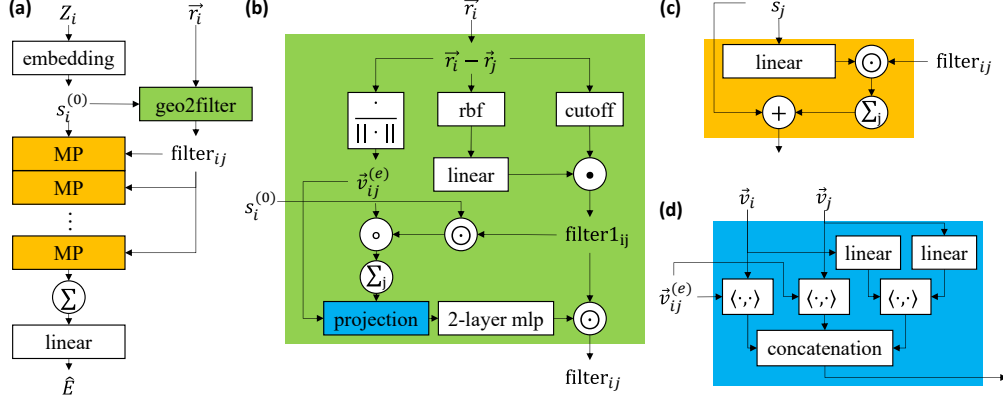


Figure 4: The architecture of GNN-LF. (a) The full architecture of GNN-LF contains four parts: an embedding block, a geo2filter block, message passing (MP) layers, and an output module. Embedding block consists of an embedding layer converting kind of atoms to learnable tensors and a neighborhood embedding block proposed by Thölke and Fabritiis [2022]. (b) The geo2filter block builds a graph with the coordinates of atoms, passes messages to produce local frames, projects vector features onto the frames, and uses edge invariant features to produce edge filters. (c) A message passing layer filters atom representations with edge filters to produce messages and aggregates these messages to update atom embeddings. (d) The projection block produces d^1, d^2, d^3 and concatenates them.

C Are orthonormal vectors necessary?

Usually, frame means a set of orthonormal vectors, while \vec{E}_i is just some vectors. A straightforward method is to use the Gram-Schmidt process. However, it leads to exploding gradients, which can be explained as follows.

$$v = LQ, \quad (43)$$

$$\frac{\partial l}{\partial v} = (L^{-1})^T \left[\frac{\partial l}{\partial Q} - \text{copyltu} \left(\frac{\partial l}{\partial Q} Q^T \right) Q \right], \quad (44)$$

where $Q \in \mathbb{R}^{3 \times 3}$ is the orthonormal vectors, $L \in \mathbb{R}^{3 \times 3}$ is the coefficients of the Gram-Schmidt process, l is the loss function, copyltu means generates a symmetric matrix by copying the lower triangle to the upper triangle. Note that L can be a singular matrix, and $(L^{-1})^T$ can make the gradient of loss explode. Moreover, the analysis before does not require the orthonormality of the frame. Therefore, we use \vec{E}_i as the local frame.

D Architecture of GNN-LF

Following Thölke and Fabritiis [2022], we also use a neighborhood embedding block which aggregates neighborhood information as the initial atom feature.

$$s_i^{(0)} = \text{Emb}_1(z_i) + \sum_{r_{ij} < r_c} \text{Emb}_2(z_j) \odot f(s_{ij}^{(e)}). \quad (45)$$

where Emb_1 and Emb_2 are two embedding layers and f is the filter function.

These special functions are proposed by previous methods [Behler and Parrinello, 2007, Unke and Meuwly, 2019].

$$\text{cutoff}(r) = \begin{cases} \frac{1}{2} \left(1 + \cos \frac{\pi r}{r_c} \right), & r < r_c \\ 0, & r > r_c \end{cases} \quad (46)$$

$$\text{rbf}_k(r_{ij}) = e^{-\beta_k (\exp(-r_{ij}) - \mu_k)^2}, \quad (47)$$

where β_k, μ_k are coefficients of the k^{th} basis.

The full architecture is shown in Figure 4. For PES tasks, the output module is a sum pooling and a linear layer. Other scalar prediction tasks can also use this module. However, on the QM9 dataset, we design special output modules for two properties. For dipole moment μ , given node representations $[s_i|i = 1, 2, \dots, N]$ and atom coordinates $[\vec{r}_i|i = 1, 2, \dots, N]$, our prediction is as follows.

$$\hat{\mu} = |\sum_i (q_i - \text{average}_j(q_j))\vec{r}_i|, \quad (48)$$

where $q_i \in \mathbb{R}$, the prediction of charge, is function of s_i . We use a linear layer to convert s_i to q_i . As the whole molecule is electroneutral, we use $q_i - \text{average}_j(q_j)$.

For electronic spatial extent $\langle R^2 \rangle$, we make use of atom mass (known constants) $[m_i|i = 1, 2, \dots, N]$. The output module is as follows.

$$\vec{r}_c = \frac{\sum_i m_i \vec{r}_i}{\sum_i m_i} \quad (49)$$

$$\langle \hat{R}^2 \rangle = |\sum_i x_i |\vec{r}_i - \vec{r}_c|^2|, \quad (50)$$

where $x_i \in \mathbb{R}$ is a scalar feature of node i . We also use a linear layer to convert s_i to x_i .

Table 4: The inference time and the GPU memory consumption of f random batches of 32 molecules (16 molecules for GemNet) from the MD17 dataset. The format is inference time in ms/GPU memory consumption in MB.

	DimeNet	GemNet	torchmd	GNN-LF	NoShare
number of parameters	2.1 M	2.2 M	1.3 M	0.8M~1.3M	2.4M~5.3M
aspirin	133/5790	612/15980	32/2065	10/279	22/883
benzene	94/1831	393/3761	33/918	8/95	11/213
ethanol	95/784	344/1565	32/532	8/54	11/115
malonaldehyde	88/784	355/1565	32/532	7/68	10/127
naphthalene	112/4470	498/11661	32/1694	9/175	15/491
salicylic_acid	92/3489	430/8182	34/1418	9/176	15/424
toluene	113/3148	423/7153	45/1322	8/176	15/458
uracil	107/1782	354/3735	32/907	8/99	14/302
average	104/2760	426/6700	34/1174	9/140	14/377

E Experiment settings

Computing infrastructure. We leverage Pytorch for model development. Hyperparameter searching and model training are conducted on an Nvidia A100 GPU. Inference times are calculated on an Nvidia RTX 3090 GPU.

Training process. For MD17/QM9 dataset, we set an upper bound (6000/1000) for the number of epoches and use an early stop strategy which finishes training if the validation score does not increase after 500/50 epoches. We utilize Adam optimizer and ReduceLROnPlateau learning rate scheduler to optimize models.

Model hyperparameter tuning. Hyperparameters were selected to minimize ll loss on the validation sets. The best hyperparameters selected for each model can be found in our code in the supplement materials. For MD17/QM9, we fix the initial lr to $1e - 3/3e - 4$, batch size to 16/64, hidden dimension to 256. The cutoff radius is selected from [4, 12]. The number of message passing layer is selected from [4, 8]. The dimension of rbf is selected from [32, 96]. Please refer to our code for the detailed settings.

Dataset split. We randomly split the molecule set into train/validation/test sets. For MD17, the size of the train and validation set are 950, 50 respectively. All remaining data is used for test. For QM9: The sizes of randomly splited train/validation/test sets are 11000, 10000, 10831 respectively.

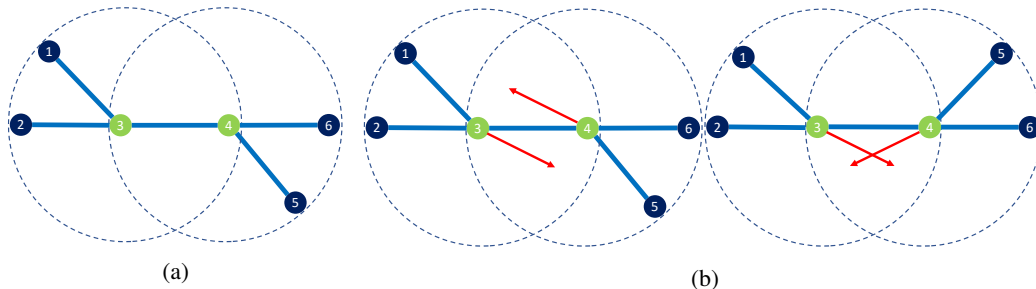


Figure 5: (a) Messages can be passed across local environments. (b) Frame-frame projection can avoid information loss in a multi-step message passing process.

F Scalability

To assess the scalability of our model, we show the inference time of random MD17 batches of 32 molecules on an NVIDIA RTX 3090 GPU. Note that GemNet consumes too much memory, and only batches of 16 molecules can fit in the GPU. Our model only takes 30% time and 12% space compared with the fastest baseline. Moreover, NoShare use 260% more space and 67% more computation time than GNN-LF with filter sharing technique.

G Passing messages across local environments

If the cutoff radius is large enough, an injective message passing layer can encode the geometry of the whole molecule. However, for computation efficiency, the local environment is usually used which contains only a proportion of atoms in the molecule. Therefore, models need several message passing layers to pass messages along a chain of neighboring atoms and across local environments to model long-range interactions. For example, in Figure 5a, though atom 5 is not in the local environment of atom 3, GNN can pass messages from atom 5 to atom 3 with two message passing layers: The first layer passes messages of atom 5 to atom 4, and the second layer send messages of atom 4, which contains information of atom 5, to atom 3.

We have proved that with a frame, a single message passing layer proposed in Proposition 4.3 can injectively encode local environments. However, some information may get lost when the message is passed along a chain of nodes by several message passing layers. For example, the two molecules are different in Figure 5b as the orientation of atom 5 changes, but GNN cannot differentiate them even if each message passing layer has the form in Proposition 4.3. It seems strange because, intuitively, atom 3 can receive message from atom 4 in the second message passing process, reconstruct the local environment of atom 4, and thus find the position change of atom 5. However, such reconstruction of the local environment is only possible when atom 3 has information about atom 4’s frame—the message sent from 4 to 3 is invariant before and after atom 5 changes its position, and the position change actually alters atom 4’s frame instead of its encoding.

Therefore, our way to solve the above information loss is very straightforward: collecting the information of neighboring nodes’ frames in the message passing process as in Equation 51.

$$\phi(\{(s_j, \vec{r}_{ij}, \vec{E}_j) | r_{ij} < r_c\}) = \rho(\sum_{r_{ij} < r_c} \varphi(\text{Concatenate}(P_{\vec{E}_i}(\vec{r}_{ij}), P_{\vec{E}_i}(\vec{E}_j), s_j))), \quad (51)$$

where $\phi(\{(s_j, \vec{r}_{ij}, \vec{E}_j) | r_{ij} < r_c\})$ aggregates information from atom i ’s local environment to atom i , \vec{E}_i means the frame of atom i , other symbols have the same meaning as in Proposition 4.3. $P_{\vec{E}_i}(\vec{E}_j)$ is the frame-frame projection.

Note that a single layer defined in Equation 51 can still encode the local environment, as extra frame-frame projection cannot lower the expressive power.

Proposition G.1. *Given a frame \vec{E} , with suitable functions ρ and φ , ϕ defined in Equation 51 encodes the local environment injectively.*

Proof. According to proposition 4.3, there exists ρ' and φ' so that $\rho(\sum_{r_{ij} < r_c} \varphi(\text{Concatenate}(P_{\vec{E}_i}(\vec{r}_{ij}), P_{\vec{E}_i}(\vec{E}_j), s_j)))$ can encode local environment injectively. Let ρ equals to ρ' , $\varphi(\text{cat}(P_{\vec{E}_i}(\vec{r}_{ij}), P_{\vec{E}_i}(\vec{E}_j), s_j)) = \varphi'(\text{cat}(P_{\vec{E}_i}(\vec{r}_{ij}), s_j))$. Then $\phi(\{(s_j, \vec{r}_{ij}, \vec{E}_j) | r_{ij} < r_c\}) = \rho'(\sum_{r_{ij} < r_c} \varphi'(\text{cat}(P_{\vec{E}_i}(\vec{r}_{ij}), s_j)))$ encodes local environment injectively. \square

Moreover, this form can solve the information loss problem in the multi-step message passing process. Given a molecule with atom coordinates $\vec{r} \in \mathbb{R}^{N \times 3}$ and atomic features (like embedding of atomic number) $s \in \mathbb{R}^{N \times d}$, let \mathcal{G} denote the undirected graph corresponding to the molecule. Node i in \mathcal{G} represents the atom i in the molecule. \mathcal{G} has edge (i, j) iff $r_{ij} < r_c$, where r_c is the cutoff radius. Let $d(\mathcal{G}, i, j)$ denote the shortest path distance between node i and j in graph \mathcal{G} . The following theorem shows that multi-step message passing can encode the full molecule injectively.

Theorem G.1. *If \mathcal{G} is a connected graph and its diameter is L , GNN with L message passing layers defined in Equation 51 can encode the $\{(s_j, \vec{r}_{ij}) | j \in \{1, 2, \dots, n\}\}$ injectively into the embedding of node i .*

Proof. We use cat to represent concatenate throughout the proof. Let $N(i)_l$ denote $\{j | d(\mathcal{G}, i, j) \leq l\}$. The l^{th} message passing layer has the following form.

$$s_i^{(l)} = \rho_l \left(\sum_{j \in N_1(i)} \varphi_l(\text{cat}(P_{\vec{E}_i}(\vec{r}_{ij}), P_{\vec{E}_i}(\vec{E}_j), s_j^{(l-1)})) \right), \quad (52)$$

where $s_i^{(0)} = s_i$.

By enumeration on l , we prove that there exist ρ_l, φ_l so that $s_i^{(l)} = \psi(\{\text{cat}(s_j, P_{\vec{E}_i}(\vec{r}_{ij})) | j \in N_l(i)\})$.

We first define some auxiliary functions.

According to [Segol and Lipman, 2020], there exists a multiset function ψ mapping a multiset of scalar to a scalar injectively. ψ can have the following form

$$\psi(\{x_i | i \in \mathbb{I}\}) = \sum_i \varphi(x_i), \quad (53)$$

where \mathbb{I} is some finite index set. As ψ is injective, it has an inverse function.

We define function m, m', m'' to extract scalar from concatenated node features.

$$m(\text{cat}(P_{\vec{E}_i}(\vec{r}_{ij}), P_{\vec{E}_i}(\vec{E}_j), s_j^{(0)})) = \text{cat}(s_j^{(0)}, P_{\vec{E}_i}(\vec{r}_{ij})). \quad (54)$$

$$m'(\text{cat}(s_j, P_{\vec{E}_i}(\vec{r}_{ij}))) = s_j. \quad (55)$$

$$m''(\text{cat}(s_j, P_{\vec{E}_i}(\vec{r}_{ij}))) = P_{\vec{E}_i}(\vec{r}_{ij}). \quad (56)$$

Last but not least, there exist a function T transforming coordinate projections from one frame to another frame.

$$T(P_{\vec{E}_i}(\vec{r}_{ij}), P_{\vec{E}_i}(\vec{E}_j), P_{\vec{E}_j}(\vec{r}_{jk})) = P_{\vec{E}_i}(\vec{r}_{ij}) + P_{\vec{E}_j}(\vec{r}_{jk})P_{\vec{E}_i}(\vec{E}_j) = P_{\vec{E}_i}(\vec{r}_{ik}) \quad (57)$$

$l = 1$: let $\varphi_1 = \varphi \circ m$, ρ_1 is identity mapping.

$l > 1$: Assume for all $l' < l$, $s_i^{(l')} = \psi(\{\text{cat}(s_j, P_{\vec{E}_i}(\vec{r}_{ij})) | j \in N_{l'}(i)\})$.

φ_l has the following form.

$$\varphi_l(\text{cat}(P_{\vec{E}_i}(\vec{r}_{ij}), P_{\vec{E}_i}(\vec{E}_j), s_j^{(l-1)})) = \varphi(\psi(\{\text{cat}(m'(x), T(P_{\vec{E}_i}(\vec{r}_{ij}), P_{\vec{E}_i}(\vec{E}_j), m''(x))) | x \in \psi^{-1}(s_j^{(l-1)})\})). \quad (58)$$

Therefore

$$\varphi_l(\text{cat}(P_{\vec{E}_i}(\vec{r}_{ij}), P_{\vec{E}_i}(\vec{E}_j), s_j^{(l-1)})) = \varphi(\psi(\{\text{cat}(s_k, P_{\vec{E}_i}(\vec{r}_{ik})) | k \in N_{l-1}(j)\})). \quad (59)$$

Note φ_l transforms coordinate projection from an old frame to a new frame.

Therefore, the input of ρ_l , namely $a_i^{(l)}$, has the following form.

$$a_i^{(l)} = \sum_{j \in N(i)} \varphi_l(\text{cat}(P_{\vec{E}_i}(\vec{r}_{ij}), P_{\vec{E}_i}(\vec{E}_j), s_j^{(l-1)})) \quad (60)$$

$$= \sum_{j \in N(i)} \varphi(\psi(\{\text{cat}(s_k, P_{\vec{E}_i}(\vec{r}_{ik})) | k \in N_{l-1}(j)\})) \quad (61)$$

$$= \psi(\{\psi(\{\text{cat}(s_k, P_{\vec{E}_i}(\vec{r}_{ik})) | k \in N_{l-1}(j)\}) | j \in N(i)\}) \quad (62)$$

We can transform $a_i^{(l)}$ to a set of set of scalars with the following function.

$$\eta(a_i^{(l)}) = \{\psi^{-1}(s) | s \in \psi^{-1}(a_i^{(l)})\}. \quad (63)$$

Therefore, $\eta(a_i^{(l)}) = \{\{\text{cat}(s_k, P_{\vec{E}_i}(\vec{r}_{ik})) | k \in N_{l-1}(j)\} | j \in N(i)\}$

We can use another function ι unions scalar sets in set \mathbb{S} to a set of scalar.

$$\iota(\mathbb{S}) = \bigcup_{s \in \mathbb{S}} s. \quad (64)$$

ρ_l has the following form.

$$\rho_l(a_i^{(l)}) = \psi \circ \iota \circ \eta(a_i^{(l)}). \quad (65)$$

Therefore, the output is

$$\rho_l(a_i^{(l)}) = \psi(\{\text{cat}(s_k, P_{\vec{E}_i}(\vec{r}_{ik})) | k \in N_l(i)\}) \quad (66)$$

Therefore, $\forall l \in \mathbb{N}$, there exists ρ_l, φ_l so that $s_i^{(l)} = \psi(\{\text{cat}(s_j, P_{\vec{E}_i}(\vec{r}_{ij})) | j \in N_l(i)\})$.

As L is the diameter of \mathcal{G} , $s_i^{(L)} = s_i^{(l)} = \psi(\{\text{cat}(s_j, P_{\vec{E}_i}(\vec{r}_{ij})) | j \in N_L(i)\}) = \psi(\{\text{cat}(s_j, P_{\vec{E}_i}(\vec{r}_{ij})) | j \in \{1, 2, \dots, n\}\})$. As ψ is an injective function, GNN with L message passing layers defined in Equation 51 can encode the $\{(s_i, \vec{r}_{ij}) | j \in \{1, 2, \dots, n\}\}$ injectively to $s_i^{(L)}$. \square

H Full ablation study of d^2

The comparison between GNN-LF with the d^2 term in Equation 9 (Dir2) and GNN-LF without d^2 term (NoDir2) is shown in Table 5. d^2 term boosts accuracy on 8/16 targets and leads to only 0.2% lower loss on average. Such negligible accuracy improvement verifies that projection of direction on the target node and frame is enough for high expressive power. This result is an indicator of the success of our theory.

I Existing methods using frame

Though some previous works [Du et al., 2022, Satorras et al., 2021, Huang et al., 2022, Luo et al., 2021] also use the term "frame" or designs similar to "frame", they are very different methods from ours.

The primary motivation of our work is to get rid of vector (a.k.a. equivariant) representation for higher and provable expressive power, simpler architecture, and better scalability. We only use vectors in the frame generation and projection process. After projection, all the remaining parts of our model only operates on scalars. In contrast, existing works [Du et al., 2022, Satorras et al., 2021, Huang et al., 2022, Luo et al., 2021] still use both vector and scalar representations, resulting in extra complexity even after using frame. For example, functions for vectors and scalars still need to be defined separately, and complex operation is needed to mix the information contained in the two

Table 5: Ablation results on the MD17 dataset. Units: energy (E) (kcal/mol) and forces (F) (kcal/mol/Å). GNN-LF does not use d^2 for some molecules, so the corresponding NoDir2 column is empty.

Molecule		Dir2	NoDir2
Aspirin	E	0.1385	0.1342
	F	0.1967	0.2018
Benzene	E	0.0708	0.0686
	F	0.1503	0.1506
Ethanol	E	0.0516	0.0522
	F	0.0798	0.0817
Malonaldehyde	E	0.0773	0.0764
	F	0.1260	0.1259
Naphthalene	E	0.1182	0.1136
	F	0.0522	0.0550
Salicylic acid	E	0.1080	0.1081
	F	0.1005	0.1048
Toluene	E	0.0931	0.0930
	F	0.0530	0.0543
Uracil	E	0.1060	0.1037
	F	0.0758	0.0751

kinds of representations. In addition, our model can beat the representative methods of this kind in both accuracy and scalability on potential energy surface prediction tasks.

Other than the different primary motivation, our model has an entirely different architecture from existing ones.

1. Generating frame: ClofNet [Du et al., 2022] produces a frame for each pair of nodes and use cross product to produce the frame. Both EGNN [Satorras et al., 2021] and GMN [Huang et al., 2022] use coordinate embeddings which are initialized with coordinates. Luo et al. [2021] initializes the frame with zero. Then these models use some schemes to update the frame. Our model uses a novel message passing scheme to produce frames and will not update it, leading to simpler architecture and low computation overhead.
2. Scalarization: Existing models [Du et al., 2022, Satorras et al., 2021, Huang et al., 2022, Luo et al., 2021] only project vector features onto the frame, while we also use frame-frame projection, which is verified to be critical both experimentally and theoretically.
3. Message passing layer: Existing models [Du et al., 2022, Satorras et al., 2021, Huang et al., 2022, Luo et al., 2021] all use both scalar and vector features and pass both scalar and vector messages, which needs to mix scalars and vectors, update scalars, and update vectors, while our model only uses scalars, resulting in an entirely different and much simpler design with significantly higher scalability.
4. Our designing tricks, including: message passing scheme to produce frame, filter decomposition, and filter sharing, are not used in [Du et al., 2022, Satorras et al., 2021, Huang et al., 2022, Luo et al., 2021]. Our experiments and ablation study verified their effectiveness.

Furthermore, existing models use different groups to describe symmetry. Du et al. [2022], Luo et al. [2021] designs $SO(3)$ -equivariant model, while our model is $O(3)$ -equivariant. We emphasize that this is not a constraint of our model but a requirement of the task. As most target properties of molecules are $O(3)$ -equivariant (including energy and force we aim to predict), our model can fully describe the symmetry.

Our theoretical analysis is also novel. Satorras et al. [2021], Huang et al. [2022], Luo et al. [2021] have no theoretical analysis of expressive power. Du et al. [2022]’s analysis is primarily based on the framework of Dym and Maron [2021], which is further based on the polynomial approximation and the group representation theory. The conclusion is that a model needs many message passing layers to approximate high-order polynomials and achieve universality. Our theoretical analysis gets rid of polynomial and group representation and provides a much simpler analysis. We also prove that one message passing layer proposed in our paper are enough to be universal.

In summary, although also using “frame”, our work is significantly different to any existing work in either method, theory, or task.

J Expressive power with symmetric input

We use the symbol in Equation 51 SchNet’s message can be formalized as follows.

$$\phi(\{(s_j, \vec{r}_{ij}, \vec{E}_j) | r_{ij} < r_c\}) = \rho(\sum_{r_{ij} < r_c} \varphi(\text{Concatenate}(s_j, r_{ij}))). \quad (67)$$

In implementation, GNN-LF has the following form.

$$\phi(\{(s_j, \vec{r}_{ij}, \vec{E}_j) | r_{ij} < r_c\}) = \rho(\sum_{r_{ij} < r_c} \varphi(\text{Concatenate}(P_{\vec{E}_i}(\vec{r}_{ij}), P_{\vec{E}_i}(\vec{E}_j), s_j, r_{ij}))). \quad (68)$$

Therefore, for all input molecules, GNN-LF is at least as expressive as SchNet.

Theorem J.1. $\forall L \in \mathbb{N}^+$, for all L layer SchNet, there exists a L layer GNN-LF produce the same output for all input molecule.

Proof. Let the following equation denote the l^{th} layer SchNet.

$$\phi'_l(\{(s_j^{(l)}, \vec{r}_{ij}, \vec{E}_j) | r_{ij} < r_c\}) = \rho'_l(\sum_{r_{ij} < r_c} \varphi'_l(\text{Concatenate}(s_j^{(l-1)}, r_{ij}))). \quad (69)$$

Let $\rho_l = \rho'_l$, $\varphi_l(\text{Concatenate}(P_{\vec{E}_i}(\vec{r}_{ij}), P_{\vec{E}_i}(\vec{E}_j), s_j, r_{ij})) = \varphi'_l(\text{Concatenate}(s_j, r_{ij}))$, which neglects the projection input.

Let the l^{th} layer of GNN-LF have the following form.

$$\phi_l(\{(s_j^{(l)}, \vec{r}_{ij}, \vec{E}_j) | r_{ij} < r_c\}) = \rho_l(\sum_{r_{ij} < r_c} \varphi_l(\text{Concatenate}(s_j^{(l-1)}, r_{ij}))). \quad (70)$$

This GNN-LF produces the same output as the SchNet. □

K How to overcome the frame degeneration problem.

As shown in Theorem 4.1, if the frame is $O(3)$ -equivariant, no matter what scheme is used, the frame will degenerate when the input molecule is symmetric. In other words, the projection degeneration problem roots in the symmetry of molecule. Therefore, we try to break the symmetry by assigning node identity features s' to atoms. The i^{th} row of s' is i . We concatenate s and s' as the new node feature $\tilde{s} \in \mathbb{R}^{N \times (d+1)}$. Let η denote a function concatenating node feature s and node identity features s' , $\eta(s) = \tilde{s}$. Its inverse function removes the node identity $\eta^{-1}(\tilde{s}) = s$.

In this section, we assume that the cutoff radius is large enough so that local environments cover the whole molecule. Let $[n]$ denote the sequence $1, 2, \dots, n$. Let $s \in \mathbb{R}^{N \times d}$ denote the scalar atomic features, $\vec{r} \in \mathbb{R}^{N \times 3}$ denote the 3D coordinates of atoms, and \vec{r}_i , the i^{th} row of \vec{r} , denote the coordinates of atom i . Let $\vec{r} - \vec{r}_i$ denote an $N \times 3$ matrix whose j^{th} row is $\vec{r}_j - \vec{r}_i$. We assume that $N > 1$ throughout this section.

Now each atom in the molecule has a different feature. The frame generation is much simpler now.

Proposition K.1. *With node identity features, there exists an $O(3)$ -equivariant function mapping the local environment $LE_i = \{(\tilde{s}_j, \vec{r}_{ij}) | j \in [N]\}$ to a frame $\vec{E}_i \in \mathbb{R}^{3 \times 3}$, and the first $\text{rank}(\vec{E}_i)$ rows of \vec{E}_i form an orthonormal basis of $\text{span}(\{\vec{r}_{ij} | j \in [N]\})$ while other rows are zero.*

Proof. For node i , we can use the following procedure to produce a frame.

Initialize \vec{E}_i as an empty matrix. For j in $[1, 2, 3, \dots, n]$, if \vec{r}_{ij} is linearly independent to row vectors in \vec{E}_i , add \vec{r}_{ij} as a row vector of \vec{E}_i .

Therefore, when the procedure finishes, the row vectors of \vec{E} form a maximal linearly independent system of $\{\vec{r}_{ij} | j \in [N]\}$.

Then, we use the Gram-Schmidt process to orthonormalize the non-empty row vectors in \vec{E} , and then use zero to fill the empty rows in \vec{E} to form a 3×3 matrix. Therefore, the first $\text{rank}(\vec{E}_i)$ rows of \vec{E}_i are orthonormal, and can linearly express all vector in $\{\vec{r}_{ij} | j \in [N]\}$. In other words, the first $\text{rank}(\vec{E}_i)$ rows of \vec{E}_i form an orthonormal basis of $\text{span}(\{\vec{r}_{ij} | j \in [N]\})$.

Note that $\vec{r}_{ij}, \vec{0}$ are $O(3)$ -equivariant vectors. Therefore, the frame produced with this scheme is $O(3)$ -equivariant. \square

With the frame, GNN-LF has the universal approximation property.

Proposition K.2. *Assuming that the node identity features are used, and the frame is produced by the method in Proposition K.1. For all $O(3)$ -invariant and translation-invariant functions $f(s, \vec{r})$, f can be written as a function of the embeddings of node 1 produced by one message passing layer proposed in Proposition 4.3.*

Proof. Let $\text{eye}_r \in \mathbb{R}^{3 \times 3}$ denote a diagonal matrix whose first r diagonal elements are 1 and others are 0.

With node identity features and method in Proposition K.1, the first $\text{rank}(\vec{E}_i)$ rows of \vec{E}_i form an orthonormal basis of $\text{span}(\{\vec{r}_{ij} | j \in [N]\})$ while other rows are zero. Especial, all vectors in $\{\vec{r}_{1j} | j \in [N]\}$ can be written as linear combination of rows in \vec{E}_1 , $\vec{r}_{1j} = w_{1j} \vec{E}_j$. Therefore, the projection operation $P_{\vec{E}_1} : \{\vec{r}_{1j} | j \in [N]\} \rightarrow \{(\vec{r}_{1j}) \vec{E}_1^T | j \in [N]\}$ is injective, as $P_{\vec{E}_1}(\vec{r}_{1j}) \vec{E}_1 = w_{1j} \vec{E}_1 \vec{E}_1^T \vec{E}_1 = w_{1j} \text{eye}_{\text{rank}(\vec{E}_1)} \vec{E}_1 = w_{1j} \vec{E}_1 = \vec{r}_{1j}$.

According to the proof of Proposition 4.3, there exists injective function ϕ so that node embeddings $z_1 = \phi(\{\tilde{s}_j, P_{\vec{E}_1}(\vec{r}_{1j}) | j \in [N]\})$. Note that both \vec{E}_1 and z_1 are functions of LE_1 .

Let τ denote a function $(z_1, \vec{E}_1) = \tau(\{\tilde{s}_j, \vec{r}_{1j} | j \in [N]\})$. $\forall o \in O(3)$, $(z_1, \vec{E}_1 o^T) = \tau(\{\tilde{s}_j, \vec{r}_{1j} o^T | j \in [N]\})$. Moreover, τ is also a invertible function because $\{\tilde{s}_j, \vec{r}_{1j} | j \in [N]\} = \{(s, p \vec{E}_1) | (s, p) \in \phi^{-1}(z_1)\}$.

Because the last column of \tilde{s} is the node identity feature, there exists an bijective function ψ converting set of features to matrix of features. $\psi(\{\tilde{s}_j, \vec{r}_{1j} | j \in [N]\}) = (s, -(\vec{r} - \vec{r}_1))$. Intuitively, it puts the features of atom with node identity i to the i^{th} row of feature matrix. Similarly, $\psi'(\{\tilde{s}_j, P_{\vec{E}_1}(\vec{r}_{1j}) | j \in [N]\}) = (s, -(\vec{r} - \vec{r}_1) \vec{E}_1^T)$.

As f is a translation- and $O(3)$ -invariant function, $f(s, \vec{r}) = f(s, \vec{r} - \vec{r}_1) = f(s, -(\vec{r} - \vec{r}_1)) = f(\psi(\{\tilde{s}_j, \vec{r}_{1j} | j \in [N]\}))$. Let $g = f \circ \psi \circ \tau^{-1}$, $g(\vec{E}_1, z_1) = f(s, \vec{r})$. Moreover, $\forall o \in O(3)$, $g(\vec{E}_1 o^T, z_1) = f(s, \vec{r} o^T) = f(s, \vec{r})$.

Let $\text{extend}(E_i) \in O(3)$ denote any matrix whose first $\text{rank}(E_i)$ rows equals to E_i 's first rows. Therefore, $f(s, \vec{r}) = f(s, \vec{r} \text{extend}(\vec{E}_1)^T) = g(\vec{E}_1 \text{extend}(\vec{E}_1)^T, z_1) = g(\text{eye}_{\text{rank}(\vec{E}_1)}, z_1) = g'(\text{rank}(\vec{E}_1), z_1)$.

Note that $\text{rank}(\vec{E}_1) = \text{rank}(\vec{r} - \vec{r}_1) = \text{rank}(P_{\vec{E}_1}(\vec{r} - \vec{r}_1)) = \text{rank}(\iota \circ \psi' \circ \phi^{-1}(z_1))$, where ι is a selection function: $\iota(z, -(\vec{r} - \vec{r}_0) \vec{E}_1^T) = -(\vec{r} - \vec{r}_0) \vec{E}_1^T$. Therefore, $f(s, \vec{r}) = g'(\text{rank}(\iota \circ \phi^{-1}(z_1)), z_1) = g''(z_1)$. \square

For simplicity, let function φ denote GNN-LF with node identity features (including adding node identity feature, generating frame, and a message passing layer proposed in Proposition 4.3), $\varphi(z, \vec{r})$ is the embeddings of node 1.

Node identity features help avoiding expressive power loss caused by frame degeneration. However, GNN-LF’s output is no longer permutation invariant. Therefore, we use the relational pooling method [Puny et al., 2022], which introduces extra computation overhead and keeps the permutation invariance.

To illustrate this method, we first define some concepts. Function $\pi : [n] \rightarrow [n]$ is a permutation iff it is bijective. All permutation on $[n]$ forms the permutation group S_n . We compute the output of all possible atom permutations and average them, in order to keep permutation invariance. We define the permutation of matrix here: for all matrix of shape $N \times m$, $\forall \pi \in S_N$, the i^{th} row of $\pi(M)$ equals to the $(\pi^{-1}(i))^{\text{th}}$ row of M .

Proposition K.3. *For all $O(3)$ -invariant, permutation-invariant and translation invariant function $f(s, \vec{r})$, there exists GNN-LF φ and some function g , with which $\frac{1}{N!} \sum_{\pi \in S_N} g(\varphi(\pi(s), \pi(\vec{r})))$ is permutation invariant and equals to $f(s, \vec{r})$.*

Proof. Define a "frame" (defined in Definition 1 in [Puny et al., 2022]) $F : V \rightarrow 2^{S_n}$, where V is the embedding space. $\forall v \in V$, $F(v) = S_n$. So the relational pooling of GNN-LF with node identity features $\langle g \circ \varphi \rangle_F(s, \vec{r}) = \frac{1}{N!} \sum_{\pi \in S_N} g(\varphi(\pi(s)), \pi(\vec{r}))$. Note that the permutation operation π and $O(3)$ operation o commute: $\pi(\vec{r}o^T) = \pi(\vec{r})o^T$. According to Theorem 2 in [Puny et al., 2022], $\langle g \circ \varphi \rangle_F$ is permutation invariant.

According to Theorem 4 in [Puny et al., 2022], if there exist function g' and φ' so that $g' \circ \varphi' = f$ (the existence is shown in Proposition K.2), there will also exist GNN-LF φ and function g , so that $\langle g \circ \varphi \rangle_F(s, \vec{r}) = f(s, \vec{r})$. \square

Therefore, we can completely solve the frame degeneration problem with the relational pooling trick and node identity features. However, the time complexity is up to $O(N!N^2)$, so we only analyze this method theoretically.

L Why is global frame more likely to degenerate than local frame?

Let $[N]$ denote the sequence 1, 2, ..., N . N is the number of atoms in the molecule.

We first consider when local frame degenerates. As shown in Theorem 4.1, the degeneration happens if and only if the local environment is symmetric under some orthogonal transformations. $\text{rank}(\vec{E}_i) < 3 \Leftrightarrow \exists o \in O(3), o \neq I, \{(s_i, \vec{r}_{ij}o^T) | r_{ij} < r_c\} = \{(s_i, \vec{r}_{ij}) | r_{ij} < r_c\}$.

The global frame has the following form,

$$\vec{E} = \sum_{i=1}^N \vec{E}_i. \quad (71)$$

We first prove some properties of \vec{E} function.

Proposition L.1. *\vec{E} is an $O(3)$ -equivariant, translation-invariant, and permutation-invariant function.*

Proof. $O(3)$ -equivariance: $\forall o \in O(3), \vec{E}_i(s, \vec{r}o^T) = \vec{E}_i(s, \vec{r})o^T$. Therefore,

$$\vec{E}(s, \vec{r}o^T) = \sum_{i=1}^N \vec{E}_i(s, \vec{r}o^T) = \left(\sum_{i=1}^N \vec{E}_i(s, \vec{r}) \right) o^T = \vec{E}(s, \vec{r})o^T. \quad (72)$$

Translation-invariance: For all translation $\vec{t} \in \mathbb{R}^3$, let $\vec{r} + \vec{t}$ denote a matrix of shape $(N, 3)$ whose i^{th} row is $\vec{r}_i + \vec{t}$. As \vec{E}_i is a function of $\vec{r}_i - \vec{r}_j = \vec{r}_i + \vec{t} - (\vec{r}_j + \vec{t})$, $\vec{E}_i(z, \vec{r} + \vec{t}) = \vec{E}_i(z, \vec{r})$. Therefore,

$$\vec{E}(s, \vec{r} + \vec{t}) = \sum_{i=1}^N \vec{E}_i(s, \vec{r} + \vec{t}) = \sum_{i=1}^N \vec{E}_i(s, \vec{r}) = \vec{E}(s, \vec{r}). \quad (73)$$

Permutation-invariance: for all permutation $\pi \in S_n$, $\pi(\vec{r})_i = \pi(\vec{r})_{\pi^{-1}(i)}$.

$$\vec{E}(\pi(s), \pi(\vec{r})) = \sum_{i=1}^N \vec{E}_i(\pi(s), \pi(\vec{r})) \quad (74)$$

$$= \sum_{i=1}^N \vec{E}_i(\{(\pi(s)_j, \pi(\vec{r})_i - \pi(\vec{r})_j) \mid |\pi(\vec{r})_i - \pi(\vec{r})_j| < r_c\}) \quad (75)$$

$$= \sum_{i=1}^N \vec{E}_i(\{(s_{\pi^{-1}(j)}, \vec{r}_{\pi^{-1}(i)} - \vec{r}_{\pi^{-1}(j)}) \mid |\vec{r}_{\pi^{-1}(i)} - \vec{r}_{\pi^{-1}(j)}| < r_c\}) \quad (76)$$

$$= \sum_{i=1}^N \vec{E}_i(\{(s_j, \vec{r}_i - \vec{r}_j) \mid |\vec{r}_i - \vec{r}_j| < r_c\}) \quad (77)$$

$$= \vec{E}(s, \vec{r}). \quad (78)$$

□

Then we prove a sufficient condition for global frame degeneration.

Proposition L.2. *rank($\vec{E} < 3$) if there exists $\vec{t} \in \mathbb{R}^3$ and $o \in O(3)$, $o \neq I$ such that $\{(s_i, \vec{r}_i - \vec{t}) \mid i \in [N]\} = \{(s_i, (\vec{r}_i - \vec{t})o^T) \mid i \in [N]\}$.*

Proof. As \vec{E} is a permutation invariant function, $\vec{E} = \vec{E}(\{(s_i, \vec{r}_i) \mid i \in [N]\})$.

As \vec{E} is a translation-invariant and $O(3)$ -equivariant function,

$$\vec{E}(\{(s_i, (\vec{r}_i - \vec{t})o^T) \mid i \in [N]\}) = \vec{E}(\{(s_i, (\vec{r}_i - \vec{t})) \mid i \in [N]\})o^T = \vec{E}(\{(s_i, \vec{r}_i) \mid i \in [N]\})o^T. \quad (79)$$

Therefore, under the condition $\{(s_i, \vec{r}_i - \vec{t}) \mid i \in [N]\} = \{(s_i, (\vec{r}_i - \vec{t})o^T) \mid i \in [N]\}$, we have

$$\vec{E}(\{(s_i, \vec{r}_i) \mid i \in [N]\})o^T = \vec{E}(\{(s_i, \vec{r}_i) \mid i \in [N]\}), \quad (80)$$

$$\implies \vec{E}(\{(s_i, \vec{r}_i) \mid i \in [N]\})(I - o^T) = 0. \quad (81)$$

Therefore, $\text{rank}(\vec{E}) + \text{rank}(I - o^T) - 3 \leq 0$. As $I \neq o^T$, $\text{rank}(I - o^T) > 0$, $\text{rank}(\vec{E}) < 3$. □

The main difference between the degeneration conditions is the choice of origin. The local frame of atom i degenerates when the molecule is symmetric with atom i as the origin point, while the global frame degenerates if the molecule is symmetric with **any origin point**. Therefore, the global frame is more likely to degenerate.

Corollary L.1. *Assume the cutoff radius is large enough so that local environments contain all atoms. If there exists i , $\text{rank}(\vec{E}_i) < 3$, then $\text{rank}(\vec{E}) < 3$.*

Proof. As $\text{rank}(\vec{E}_i) < 3$, $\exists o \in O(3)$, $o \neq I$, $\{(s_j, (\vec{r}_i - \vec{r}_j)o^T) \mid j \in [N]\} = \{(s_j, (\vec{r}_i - \vec{r}_j)) \mid j \in [N]\}$.

Therefore,

$$\{(s_j, -(\vec{r}_i - \vec{r}_j)o^T) \mid j \in [N]\} = \{(s_j, -(\vec{r}_i - \vec{r}_j)) \mid j \in [N]\} \quad (82)$$

$$\implies \{(s_j, (\vec{r}_j - \vec{r}_i)o^T) \mid j \in [N]\} = \{(s_j, \vec{r}_j - \vec{r}_i) \mid j \in [N]\} \quad (83)$$

Let $\vec{t} = \vec{r}_i$, according to Proposition L.2, $\text{rank}(\vec{E}) < 3$. □

Therefore, when the cutoff radius is large enough, the global frame will also degenerate if some local frame degenerates.